

Annual Review of Fluid Mechanics

Fluid Mechanics Challenges in Direct-Ink-Writing Additive Manufacturing

Alban Sauret,¹ Tyler R. Ray,² and Brett G. Compton³

Annu. Rev. Fluid Mech. 2026. 58:413-42

The *Annual Review of Fluid Mechanics* is online at fluid.annualreviews.org

https://doi.org/10.1146/annurev-fluid-100224-

Copyright © 2026 by the author(s). All rights reserved

Keywords

direct-ink writing, rheology, suspensions, nozzle clogging, printability, fluid instabilities, liquid filament, additive manufacturing, 3D printing

Abstract

Direct-ink writing (DIW) has rapidly become a versatile 3D fabrication method due to its ability to deposit a wide range of complex fluids into customizable 3D geometries. This review highlights key fundamental fluid mechanics and soft matter challenges across the different stages of the DIW printing process. The rheology of fluids and suspensions governs the flow behavior through narrow nozzles, posing questions about extrudability, confined flow dynamics, and clogging mechanisms. Downstream, the formation and deposition of extruded filaments involve extensional flows and potential instabilities, while postdeposition dynamics introduces complexities related to yield stress and structural stability. These stages are inherently interdependent, as optimizing material composition without considering filament stability risks compromising the final structure. As DIW applications expand through advanced ink formulations, developing fundamental fluid mechanics frameworks is essential to replace trial-and-error approaches with predictive design methodologies to enable more precise control over and reliability of the printing process.

¹Department of Mechanical Engineering; Department of Chemical and Biomolecular Engineering, University of Maryland, College Park, Maryland, USA; email: asauret@umd.edu

²Department of Mechanical Engineering; Department of Cell and Molecular Biology, John A. Burns School of Medicine, University of Hawaiʻi at Manoa, Honolulu, Hawaii, USA; email: raytyler@hawaii.edu

³Department of Mechanical and Aerospace Engineering; Department of Materials Science and Engineering, University of Tennessee, Knoxville, Tennessee, USA; email: brettcompton@utk.edu

Filament: a single line of deposited material; also called a road in fused filament fabrication to distinguish the printed line from the feedstock filament

Material extrusion:

the ISO/ASTM 52900 standard term and acronym for AM processes that selectively deposit material through a nozzle or orifice

Direct-ink writing (DIW): sometimes referred to as robocasting, paste extrusion modeling, or solvent-cast AM

Robocasting:

a portmanteau of "robotic slip casting"; usually connotes material extrusion of a ceramic or metal particle suspension

Viscoelastic fluid: a fluid that exhibits both elastic and viscous properties

1. INTRODUCTION

1.1. Direct-Ink Writing: Principle and Challenges

Additive manufacturing (AM) enables the fabrication of objects with unprecedented design freedom while simultaneously reducing material waste (Gibson et al. 2021). Unlike traditional subtractive methods, AM builds parts layer by layer from a material library spanning thermoplastic filaments, complex fluids, powders, and solid metal feedstocks. Industries such as aerospace, bioengineering, and construction have adopted AM processes to produce lightweight, intricate, and robust structures and rapidly prototype components (Murphy & Atala 2014, Buswell et al. 2018, Najmon et al. 2019).

Material extrusion has emerged as one of the most versatile of the AM processes owing to the capacity to process high-viscosity fluids and create near-net-shape components (Frazier 2014, Ngo et al. 2018). In this review, we focus on direct-ink writing (DIW), also known as robocasting, which is an extrusion-based process that operates at or near room temperature, dispensing complex fluids through a nozzle without relying on melting (Cesarano 1998). DIW inks solidify via alternative mechanisms such as cross-linking, gelation, and solvent evaporation (Lewis 2006, Wilt et al. 2021). This approach enables the use of a wide range of complex fluids as feedstocks ranging from thermoset polymers and biomaterials to ceramic- or metal-particle-laden slurries (Saadi et al. 2022). Alongside relevance in material science, DIW has broad utilization in concrete 3D printing (Bos et al. 2016), forming cellular materials (Tian & Zhou 2020), and biofabrication (Groll et al. 2016), where tissue engineering applications are steadily advancing (Malda et al. 2013). Figure 1 provides some DIW examples that highlight the wide range of materials, shapes, and scales possible with this technique.

This process, in combination with the complex fluids involved, introduces fluid mechanics and soft matter challenges that span multiple length scales and timescales at different stages of the process. The typical flow rates and nozzle diameters in DIW are usually larger than those in inkjet printing (Derby 2010, Lohse 2022), but the influence of the rheology of the fluid on the overall process can be just as pronounced and govern the printability of a given material (Larson 1999, Lewis 2006, Rau et al. 2023). The complex fluids used in DIW are typically shear-thinning, yield-stress, viscoelastic fluids or suspensions, whose rheological properties must be tuned so that they flow readily under high shear in the nozzle yet rapidly recover a solid-like state upon deposition to resist spreading or sagging. This inherent complexity introduces fluid mechanics challenges in optimizing both the print quality and the process throughput.

1.2. Overview of the Direct-Ink-Writing Process

Figure 2 shows a simplified overview of the key DIW process stages. Although interdependent, they can be broadly separated into four main steps, each presenting distinct fluid mechanics challenges. These complex phenomena are often characterized using a set of dimensionless parameters that compare the relative importance of various physical effects (see the sidebar titled Dimensionless Parameters).

1.2.1. Fluid extrusion and flow in the nozzle. Extrusion of the ink is usually achieved via volumetric pumps, leadscrew-driven plungers, or air pressure. In practice, many DIW researchers prefer air pressure to drive the flow, as this is clean, cheap, and fast. However, this approach lacks precise control over the flow rate, which is often tuned during the printing process by manually adjusting the air pressure. Flow rate in air-pressure-driven DIW is sensitive to changes in back pressure that can arise due to variations in material viscosity, nozzle geometry, or even layer height, and the system is susceptible to clogging. On the other hand, volumetric pumps offer precise



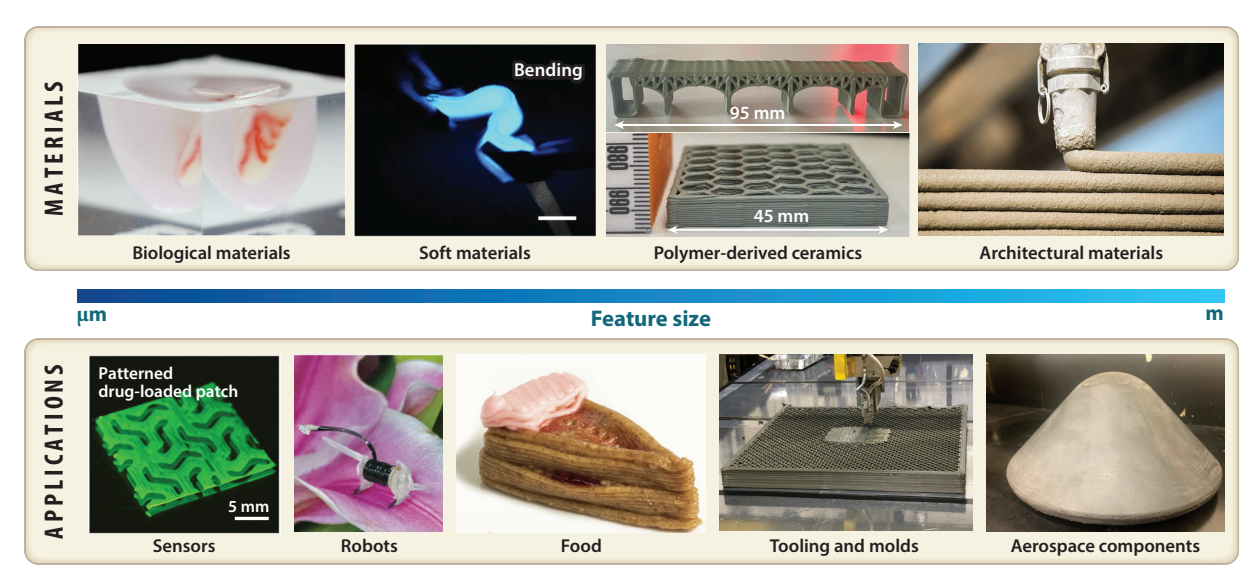


Figure 1

Representative examples of both materials and applications that highlight the breadth of direct-ink writing (DIW). The DIW process supports printing from a variety of feedstocks spanning biological materials (e.g., cells, tissue constructs), soft materials (e.g., polymers), polymer-derived ceramics, and architecture- or construction-relevant materials (e.g., concrete). This expansive material library supports an equally broad range of applications, including sensors/medicine, robots, food, tooling and molds, and aerospace components. Photos reproduced from (top, left to right) Skylar-Scott et al. (2019) (CC BY-NC 4.0, with permission), Zhang et al. (2022) (CC BY 4.0), Compton et al. (2025), and ICON Technology, Inc. (with permission, photo credit: Regan Morton); (bottom, left to right) Wu et al. (2024) (CC BY 4.0), Zhu et al. (2023) (with permission; copyright 2023 American Chemical Society), Blutinger et al. (2023) (CC BY 4.0), Romberg et al. (2022b) (with permission), and Bouslog et al. (2021) (public domain, NASA).

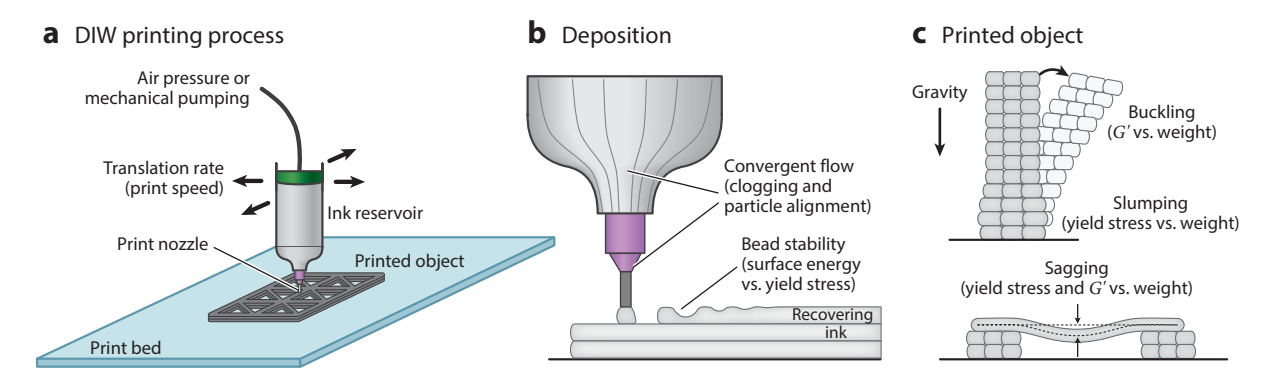


Figure 2

Schematic of the direct-ink-writing (DIW) process and key phenomena influencing success or failure. (a) General schematic illustrating the overall process components. (b) The deposition process includes regions of convergent flow where the shear rate increases. Convergent flow is effective at aligning particles, if present in the ink, but constrictions are also problematic areas for clogging in highly loaded inks. The balance of surface tension to yield stress and recovery time of the ink will dictate stability and wetting of the underlying layers. (c) In the final printed structure, the yield stress and storage modulus of the ink must counteract the effects of gravity to prevent slumping of lower layers, buckling of tall slender objects, and sagging of spanning features to maintain the printed shape prior to and during curing, drying, or solidification.

DIMENSIONLESS PARAMETERS

Various dimensionless numbers help characterize DIW processes. Although extrusion flows in DIW tend to involve highly viscous fluids at low or moderate speeds, the Reynolds number $Re = \rho UD/\eta$, which compares inertial and viscous effects, remains useful as high-speed extrusion can introduce instabilities.

Inks exhibit complex rheological properties such as shear thinning and yield stress, leading to the Bingham number $Bn = \tau_Y D/\eta U$, which compares the yield stress τ_Y to the viscous stress $\eta U/D$. For low Bn, the fluid behaves like a liquid, whereas at high Bn, the yield stress dominates and a pressure must first overcome τ_Y before any flow occurs. The viscoelastic properties are characterized by the Deborah number $De = \lambda/\tau$ and the Weissenberg number $Wi = \dot{\gamma}\lambda$, where λ is the viscoelastic relaxation time, τ the characteristic time of the external process, and $\dot{\gamma}$ the shear rate. Particles are commonly added to the fluid to bring additional properties to the final materials, and an important parameter to predict clogging is the ratio of the nozzle diameter to particle size: $\alpha = D/d_p$. When α is too small, clogging is common.

Once the ink is extruded from the nozzle, it transitions from confined to free-surface flow, resulting in a complex interplay of viscous, inertial, capillary, and gravitational forces. The Weber number, $We = \rho U^2 D/\gamma$ characterizes the ratio of inertial to capillary forces and thus whether the ligament necks and pinches off. We is often small in DIW, leading to stable continuous ligaments, but it can become significant at high extrusion rates. The capillary number $Ca = \eta U/\gamma$ compares the viscous stress with the surface tension effects. A combination of the Weber number and Reynolds number defines the Ohnesorge number $Ob = We^{1/2}/Re$, frequently used for jetting processes.

The Bond number $Bo = \rho g L^2/\gamma$ represents the ratio of gravitational to capillary forces, where L is the length scale of the filament or printed structure. Bo is relevant for larger nozzle diameters or tall structures. For yield-stress fluids, excessive spreading can be mitigated by tuning the yield stress, τ_Y , to overcome capillary and gravitational forces, which can be captured through a printability number $\Xi = \tau_Y/(\gamma/D + \rho g L)$. $\Xi > 1$ favors self-support against both capillary retraction and gravity. For low Bond numbers, i.e., the capillary-dominated regime, Ξ reduces to a plastocapillary number $\mathcal{J} = \tau_Y L/\gamma$, commonly used to set the minimum yield stress for vertical build fidelity.

As the deposited filament recovers, dries, or changes temperature, additional physical phenomena come into play, leading to more dimensionless numbers. For instance, the Péclet number Pe quantifies the relative importance of advective to diffusive transport, the Schmidt number Sc compares the ratio of momentum diffusivity ν to mass diffusivity $D_{\rm diff}$, and the Nusselt and Biot numbers compare heat conduction to convection at an interface. When temperature gradients affect viscosity or curing rates, the Prandtl number, $Pr = \nu/\kappa$, describes their ratio. If chemical reaction rates such as cross-linking or curing occur, the Damköhler number compares their rate to the mass transport rate.

control over the flow rate, but they are expensive, slow to load, and laborious to clean out. They offer more robust DIW printing but are not impervious to clogging and can damage delicate inks like cell-laden bio-inks or foams (Pack et al. 2020). In both cases, the flow of the complex fluids within the nozzle is a critical stage governed by the ink's rheology, the design of the nozzle, and potential clogging when particles are present.

- **1.2.2.** Filament formation and initial deposition on the substrate. Upon exiting the nozzle, the fluid transitions from a confined to a free-surface flow, forming a filament (see the sidebar titled Embedded Direct-Ink Writing for the embedded-printing variant). The geometry depends on the interplay between driving pressure, flow rate, distance from the substrate, and rheological parameters. Unsteady extrusion, or the relative velocity between the nozzle and the substrate, may cause diameter fluctuations, unintended breakups, or coiling of the filament on the substrate.
- **1.2.3. Short-time evolution of the filament on the substrate.** Once the fluid contacts the substrate, its spreading, leveling, and interlayer bonding become important issues. Low-viscosity



EMBEDDED DIRECT-INK WRITING

For the DIW process discussed in this review, the ink filament is deposited layer by layer in air onto a substrate. By contrast, embedded DIW deposits material into a supporting fluid, rather than in air, which provides uniform, omnidirectional support (Wu et al. 2022). This approach facilitates the deposition of low-viscosity fluids that would otherwise slump or drip in air. Selection of a support fluid can be based upon desirable yield-stress properties or for neutral buoyancy in order to tailor fluid-fluid interfacial effects and mechanical support. For example, embedded DIW has been widely adopted in biofabrication to print hydrogels or cell-laden inks (Hinton et al. 2015), enabling the production of complex tissue scaffolds that mimic soft biological structures or facilitating the manufacturing of sensors (Muth et al. 2014).

The difference in support (fluid versus air) results in some effects discussed in this review becoming negligible, while other effects remain relevant. For example, large-scale flow instabilities, such as sagging or buckling, become negligible relative to open-air DIW, as the supporting fluid confines the extruded ligament. Challenges such as clogging with suspensions or nozzle flow instabilities, such as die swell or erratic pulsations, when utilizing viscoelastic inks or high flow rates, can affect both embedded and open-air DIW printing. The use of a supporting fluid also introduces new fluid mechanics challenges for embedded DIW. For instance, a bath made of a yield-stress fluid undergoes localized yielding around the moving nozzle. It must briefly flow as the nozzle passes, then rapidly resolidify to entrap the newly deposited filament (Grosskopf et al. 2018). Another particularity is that fluid-fluid interfacial dynamics govern whether the printed filament remains stable or breaks into droplets (Friedrich & Seppala 2021). The bath rheology and self-healing also play an important role in stabilizing small features, thereby impacting achievable resolution and part fidelity. Embedded DIW also enables the simulation of microgravity conditions on Earth, offering a platform to study AM in near-zero-gravity environments (Kauzya et al. 2024).

fluids may spread or drip excessively, undermining shape fidelity, while highly viscous or yieldstress inks can maintain shape but risk incomplete wetting or poor interlayer adhesion.

1.2.4. Postdeposition solidification or curing. The deposited material solidifies via solvent evaporation, cross-linking, thermal cooling, or other mechanisms (Nelson et al. 2019). The speed and extent of solidification directly affect the mechanical properties and interlayer adhesion.

1.3. A Fluid Mechanics and Soft Matter Perspective

DIW relies on the precise manipulation of complex fluids, and the process spans fundamental fluid mechanics concepts, such as nozzle flow, clogging, ligament formation, deposition, and slumping, along with interfacial dynamics and soft matter physics concepts, such as extensional instabilities and viscous coiling. Unlike conventional Newtonian liquids, DIW inks often consist of a dispersed phase (e.g., particles, fibers, biological cells) in a non-Newtonian carrier fluid. Much of the progress in DIW has been empirically driven by application-specific needs (Ngo et al. 2018) in areas such as 3D food printing (Lee et al. 2024), construction (Paolini et al. 2019, Mechtcherine et al. 2020, Schild et al. 2024), metallic and ceramic part production (Rane & Strano 2019), medicine (Culmone et al. 2019, Tay et al. 2023, Hou et al. 2024, Ho et al. 2025, Zhao et al. 2025), and bio-ink printability (Schwab et al. 2020). Printability maps correlate some rheological or process parameters with successful printing, yet the interplay of these factors, particularly with particulate suspensions, raises many fundamental fluid mechanics questions (Pandya et al. 2023, De Smedt et al. 2025). For instance, complex phenomena such as clogging, dispersion stability, and capillary effects on the substrate have a critical impact on filament formation and interlayer bonding.

Printability map: correlates material properties and process parameters with successful printing outcomes



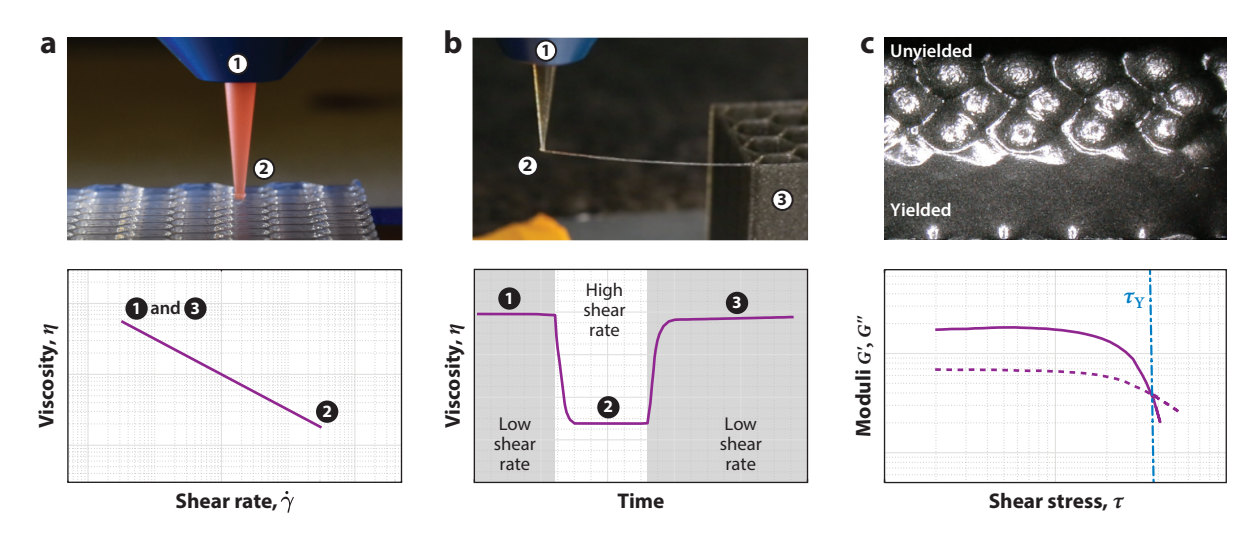


Figure 3

Illustration and schematics of the rheological requirements at different steps of the direct-ink-writing process: (a) shear-thinning behavior during extrusion, (b) thixotropy once deposited on the substrate, and (c) yield stress to avoid slumping. ① refers to the ink inside the syringe before extrusion (low shear), ② corresponds to the high shear observed during extrusion through the nozzle, and ③ refers to the postdeposition situation (low shear), where the ink recovers its structure. In the top panel of c, the image shows the end view of a flexural bar printed using a low-yield-stress ink, showing slumping and coalescence of the lower layers. Panel c, top adapted from Compton et al. (2018).

Extracting and systematically translating core fluid mechanics phenomena into predictive models is crucial for minimizing trial and error during the various stages of the process and enabling predictive design strategies for next-generation DIW applications. Engineers typically adjust ink rheology, flow parameters, nozzle diameter, and printing velocity until parts of acceptable quality are produced (Ngo et al. 2018). While numerous reviews address DIW from application-specific perspectives, they typically emphasize process engineering over the underlying physics and fluid mechanics phenomena governing the printing process (e.g., Zocca et al. 2015, Placone & Engler 2018, Tagliaferri et al. 2021, Tay et al. 2023, Hou et al. 2024, Ho et al. 2025, Zhao et al. 2025). These limitations become even more evident in multiphase systems as, for instance, a suspension displaying fluid-like behavior in bulk rheometry may undergo abrupt clogging near the nozzle tip when particles bridge.

This empirical approach lacks predictive power for critical failures like nozzle clogging, filament fracture, and structural collapse. The goal of this review is to discuss DIW challenges across diverse material systems and scales through the lens of fluid mechanics, aiming to support establishing a theoretical foundation that can guide material selection, nozzle geometry optimization, and process parameter determination. Beyond practical applications, the inherent complexity of DIW can also inspire various fundamental fluid mechanics problems involving complex fluids.

2. RHEOLOGICAL CONSIDERATIONS AND PRINTABILITY

2.1. Rheological Design Principles

In DIW, a complex fluid must flow through the nozzle under pressure like a viscous fluid and must be stable under elongation as a filament, yet it must also hold its shape like an elastic solid once deposited. **Figure 3** illustrates schematically key rheological requirements at different successive stages of the DIW process: low shear inside the syringe before extrusion, high-shear environment

when flowing through the nozzle, and the postdeposition stage at low shear, during which the ink must rapidly recover its structure to retain its shape. Satisfying this multifaceted rheological profile presents significant challenges, particularly when incorporating solid particles. As a result, a central challenge in DIW lies in designing complex fluids, or inks, that satisfy these multiple rheological and mechanical criteria throughout the printing process. The dual requirements of extrudability and shape retention collectively define the printability of a material (Agrawal & García-Tuñón 2024). Unlike other classical flow processes that may optimize rheology for a single flow regime, DIW requires simultaneous control over shear-thinning, viscoelasticity, yield stress, and thixotropy across rapidly changing timescales (Lewis 2006). While comprehensive reviews have specifically addressed DIW fluid rheology (e.g., Rau et al. 2023, Wei et al. 2023, De Smedt et al. 2025) and guidelines exist for designing complex fluids (Ewoldt & Saengow 2022), we focus here on summarizing the key rheological aspects and the corresponding parameters that are used in the following sections of the review.

2.1.1. Yield stress and shape retention. A finite yield stress τ_Y is crucial for self-supporting prints. Yield-stress fluids, such as colloidal gels and cementitious materials, flow only when the stress exceeds a critical threshold τ_Y ; otherwise, they behave as an elastic solid (Coussot 2005, Balmforth et al. 2014, Dinkgreve et al. 2016, Bonn et al. 2017). For successful extrusion, τ_Y must be low enough to permit flow under practical pressures but large enough to overcome both gravitational forces and surface tension effects that would otherwise deform the printed structure (Pashias et al. 1996). Common DIW inks typically exhibit τ_Y values ranging from 10^1 to 10^3 Pa, which are sufficient to support millimeter-sized features. However, excessive yield stress presents other challenges: Inks that are too solid-like may resist extrusion at operational pressures or fail to merge properly with previously deposited layers. The printability index, discussed later, can offer guidance for formulating inks with optimal τ_Y values.

2.1.2. Shear-thinning behavior. Most DIW inks are formulated to be shear-thinning fluids, where viscosity decreases with an increasing shear rate. This rheological behavior is important, as the ink is very viscous or paste-like under low or zero shear (e.g., in the syringe and after deposition). As the ink flows through the nozzle, it experiences a high shear rate ($\dot{\gamma} \sim 10^2 - 10^3$ Pa), which leads to a reduction in viscosity, thereby enabling extrusion without requiring excessive pressure. Upon deposition, the viscosity rapidly rises as the shear rate decreases (i.e., at low $\dot{\gamma}$) and stabilizes the filament geometry. In contrast, a purely Newtonian ink with constant viscosity would be either too viscous for practical extrusion or too fluid to maintain structural integrity once deposited. The shear-thinning behavior typically originates from jammed microstructures that yield and break down under applied shear (Nelson & Ewoldt 2017).

A classical rheological model used for DIW inks is the Herschel-Bulkley model,

$$\tau = \tau_{\rm Y} + K \dot{\gamma}^n, \qquad 1.$$

where τ is the shear stress, $\dot{\gamma}$ is the shear rate, K is a consistency coefficient, and n is the flow index (0 < n < 1 for shear-thinning fluids) (Balmforth et al. 2014). Many DIW inks exhibit Herschel–Bulkley behavior with notably small n values, indicating high shear-thinning properties. While alternative constitutive models exist, including Bingham plastic, Casson fluid, or Carreau models, the Herschel–Bulkley model remains a convenient and widely adopted approach in DIW research.

2.1.3. Thixotropy and recovery. Beyond shear-dependent viscosity and yield stress, DIW inks typically exhibit thixotropic behavior in which the microstructure, and thus viscosity, rebuilds over time. In oscillatory rheology, the storage modulus G' quantifies the elastic, energy-storing response of the fluid, while the loss modulus G'' quantifies the viscous, energy-dissipating response. These complementary moduli are useful indicators of how quickly an ink recovers its solid-like structure

Yield-stress fluid:

a material that resists deformation like a solid until the applied shear stress exceeds a specific threshold; beyond the critical yield stress, it flows

Shear-thinning fluid:

the shear viscosity of the fluid decreases as the imposed shear rate or shear stress is increased

Thixotropy:

time-dependent property in which the viscosity of the fluid decreases when subjected to shear stress and then gradually recovers when the stress is removed

after extrusion. For DIW applications, a thixotropic ink that recovers quickly after shear is highly desirable. During printing, the ink undergoes high shear within the nozzle, breaking down the internal structure. Upon deposition, rapid recovery of solid-like properties helps maintain the printed form. A standard experimental approach to probe this behavior is measuring G' (or the viscosity) through a three-stage protocol: (a) initial low-shear characterization, (b) application of a high-shear condition that simulates extrusion, and (c) return to low shear to track the G' (or the viscosity) recovery kinetics. Printable inks generally recover a large fraction of their original G', relative to G'', within a short time. In practice, a good printability requires a balanced thixotropy, since the ink must rebuild its internal structure quickly enough after extrusion to maintain the shape of the filament, yet not so quickly that it clogs the nozzle or compromises interlayer adhesion (Rau et al. 2023).

2.1.4. Viscoelasticity and extensional rheology. Viscoelastic inks introduce time-dependent behavior through molecular entanglements or transient networks. A high Deborah number De can stabilize filaments via elastic recoil but also induce die swell, distorting printed features (Ouyang et al. 2020). For instance, PDMS (polydimethylsiloxane) inks with a relaxation time of $\lambda \sim 1 \, \text{s}$ exhibit controllable swell at high extrusion speeds ($\tau \sim 0.1$ s, where τ is the process timescale), while slower rates ($\tau \sim 10$ s) minimize elastic effects.

In addition to shear-dominated flows, the fluid may also experience strong extensional deformation within and upon exiting the nozzle. As a result, the extensional viscosity, defined as the tensile stress divided by the extensional strain rate, plays a critical role in DIW during the formation of the filament and for its stability (Münstedt 2018, Nelson et al. 2018). Sufficient extensional resistance helps filaments span small gaps or maintain cohesion, yet if it is too large, extruded filaments may fail to detach cleanly. Although quantifying extensional properties is challenging (Tirtaatmadja & Sridhar 1993), these effects significantly influence print fidelity.

2.1.5. Particle-laden inks: rheology of particulate suspensions. DIW inks often contain dispersed solid particles to achieve desirable mechanical and flow properties. Highly loaded particle suspensions ($\phi > 0.4$) present unique rheological challenges in DIW printing (Marnot et al. 2023). As the volume fraction ϕ approaches the jamming threshold ϕ_{max} , viscosity increases rapidly.

The sharp divergence of the viscosity necessitates precise pressure control during printing. Particle size distribution also plays a role, as bimodal distributions can increase ϕ_{max} and decrease viscosity for a volume fraction (Pednekar et al. 2018, Delarue et al. 2024). In general, as the volume fraction increases, one needs to consider the rheology of these complex suspensions, particularly as particle-particle interactions become more important. We point the reader to different review articles on the rheology of suspensions, such as those by Stickel & Powell (2005), Mewis & Wagner (2011), and Guazzelli & Pouliquen (2018), among others, which provide additional details beyond the scope of this review. We should emphasize that many fundamental questions on suspension flows remain poorly studied or unexplored, including the rheology of suspensions made of polydisperse or of nonspherical particles, the behavior of suspensions at interfaces, their extensional rheology, and suspensions whose particles are dispersed in non-Newtonian interstitial fluids.

2.2. Printability Map

Because DIW involves multiple parameters (material rheology, nozzle size, pressure, speed, etc.), printability maps are often useful to visualize the operating window in which printing is successful (Chan et al. 2020, García-Tuñón et al. 2023, Saengow et al. 2025). In a printability map, relevant material properties or process parameters are plotted against each other, and different regions are marked to indicate whether the outcome is a successful print or a failure mode. Usually, these



maps are created by systematically varying the rheological properties of the fluid and the printing conditions and empirically observing the outcome. This empirical approach illustrates the need for more predictive tools in DIW.

Some studies have, nevertheless, introduced dimensionless groups to predict regions of a printability map. For instance, M'barki et al. (2017) have shown that the role of τ_Y on the final stability can be described through a dimensionless printability number,

$$\Xi \equiv \frac{\tau_Y}{\gamma D^{-1} + \rho g b},$$
 2.

where D is the nozzle diameter, γ is the surface tension, and ρgh is the weight of the object. Stable printing requires fulfillment of the condition $\Xi > 1$, which corresponds to the situation where the yield stress overcomes both gravitational stress and capillary pressure to prevent deformation.

3. FLOW AND CLOGGING IN THE NOZZLE

3.1. Flow of Complex Fluids in Nozzles

In DIW, the viscous fluid is forced through a nozzle, often at low Reynolds numbers, so that inertia is usually negligible, and the flow rate responds quasi-instantaneously to the applied pressure. Whereas for Newtonian fluids, the volumetric flow rate Q is proportional to the pressure drop ΔP , for more complex rheological properties, such as shear thinning, the pressure–flow rate relationship deviates from a simple linear law (Li et al. 2011, Boyko & Stone 2021). In the nozzle, increasing ΔP drives higher shear near the walls and thus lowers the effective viscosity. In addition, the presence of a yield stress requires a minimum pressure to initiate flow, $Q \propto (\Delta P - \Delta P_y)^m$. As a result, DIW inks often exhibit a critical pressure to initiate extrusion, followed by a quick rise in flow rate beyond this pressure.

The convergence from a syringe or a reservoir into a small nozzle induces a flow field where extensional flow is dominant near the centerline and shear-dominated flow is observed close to the walls. If the convergence is too abrupt, recirculation zones can arise, increasing the pressure drop required to maintain the same flow rate (Baloch et al. 1996, Alves et al. 2004). For viscoelastic fluids, elastic stresses further enhance the pressure drop. Various studies have reported an extra pressure difference in convergent flows that exceeds the Newtonian prediction (e.g., Rothstein & McKinley 2001, Aguayo et al. 2008). This additional pressure drop requires higher operational pressures and can induce unwanted flow instabilities or excessive shear that may compromise the microstructure of the ink, for instance, breaking polymer chains or damaging cells in bio-inks.

It is thus desirable to optimize nozzle shapes to minimize the pressure drop and allow greater flow control. For instance, Schuller et al. (2024) used a computational fluid dynamics (CFD)-based optimization algorithm to determine the ideal nozzle-contraction shape for different viscoelastic constitutive models. Their results showed that modest variations of the contraction angle and inlet radius can significantly reduce extensional stresses while maintaining throughput. However, a geometry optimized for one rheology may not be optimized for another. Adjusting curvature or streamwise length of the nozzle may selectively promote shear or extension, depending on whether the goal is, for instance, to align particles, minimize pressure drop, or encourage a particular flow pattern. These optimization approaches could be extended to particulate suspensions, where additional constraints, such as particle alignment or clogging, come into play. For example, a longer extensional zone might promote the alignment of anisotropic particles in shear-thinning fluids (Férec et al. 2016).

Feret diameter: measure of a particle size along a specified direction

3.2. Suspensions of Particles and Clogging of Nozzles

One of the attractive features of DIW is the ability to utilize dense suspensions as inks. Highly loaded suspensions of ceramic or metal powders enable the printing of green bodies that undergo minimal drying shrinkage and have a high relative density, highly loaded polymer resins enable the printing of high-performance composites and syntactic foams, and high loading of functional fillers (e.g., magnetic particles, dielectric material, radiation absorbers, conductive fillers) leads to composites with higher performance in the intended application. A synergistic benefit of large volume fractions of particles is that high loading of filler materials in a carrier fluid can impart the shear-thinning and yield-stress behavior that is desirable in DIW inks. However, a large volume fraction of particles can also lead to clogging, which is a key bottleneck to achieving reliable and defect-free DIW prints. While complete clogging leads to the end of the print, partial clogging results in flow or volume fraction variations. The consequences of nozzle clogging extend beyond process disruption, which often necessitates stopping to clear or replace the nozzle. Clogging also leads to variability in extrusion rate, resulting in poor layer uniformity, high internal pressures generating mechanical stress on the extruder mechanism, and potential variations in the extruded filament thickness. Although a common issue, our understanding of clogging by particulate suspensions in narrow nozzles remains largely empirical. Indeed, it is natural in material science to try to avoid rather than document clogging, and it is a difficult phenomenon to observe in situ. As a result, assessing potential nozzle clogging currently relies on empirical rules of thumb, such as reducing the volume fraction of particles or increasing the nozzle diameter, rather than systematic fluid mechanics principles. Such an approach inherently limits the complexity and functionality of future ink formulations, requiring a high solid content for structural or functional performance.

3.2.1. Clogging mechanisms. In DIW, nozzles of diameters of order 100 µm-1 mm are used to extrude suspensions of particles of various sizes and volume fractions up to 60%, which can lead to clogging through different mechanisms: sieving, bridging, and deposition on nozzle walls (Dressaire & Sauret 2017, Dincau et al. 2023).

Sieving is a size-exclusion mechanism. Particles, or agglomerates of particles, of dimension d larger than the nozzle diameter D cannot pass and thus clog the constriction (Sauret et al. 2014, Delouche et al. 2020). In the case of anisotropic particles, such as fibers, the occurrence of sieving also depends on the orientation of the particles. Often, the largest Feret diameter, e.g., the length for a fiber, can be considered as the length scale (Duchêne et al. 2020, Bräsel et al. 2024). Sieving can occur even for particles much smaller than the nozzle dimension when transient clusters form, as observed, for instance, with irregularly shaped fillers, inadequately dispersed agglomerates, or flocculation-prone chopped fibers (Villalba et al. 2023). This can happen for colloidal particles that are not well-stabilized and form clusters, or flocs, that are effectively much larger than the nominal particle size and larger than the nozzle diameter. Even if the dimension of a deformable particle is larger than the nozzle size, the particle may still flow through if the applied pressure is large enough to deform it sufficiently (Moore et al. 2023).

Bridging occurs when particles of dimensions smaller than, but comparable to, the nozzle diameter form a stable arch across the constriction (Marin & Souzy 2024). Most fundamental studies on bridging have been performed with spherical particles and showed that bridging is probabilistic, as it requires a sufficient number of particles to span the constriction to arrive together in the correct configuration (Goldsztein & Santamarina 2004). The probability of bridging increases as the volume fraction increases (Vani et al. 2022) or as the nozzle-to-particle size ratio decreases (Marin et al. 2018). For clogging by bridging, the mechanical properties of the particles play an important role, as increasing the effective interparticle friction stabilizes arches and therefore raises the probability of bridging (Hsu et al. 2021). Bridging can also occur with nonspherical particles, such

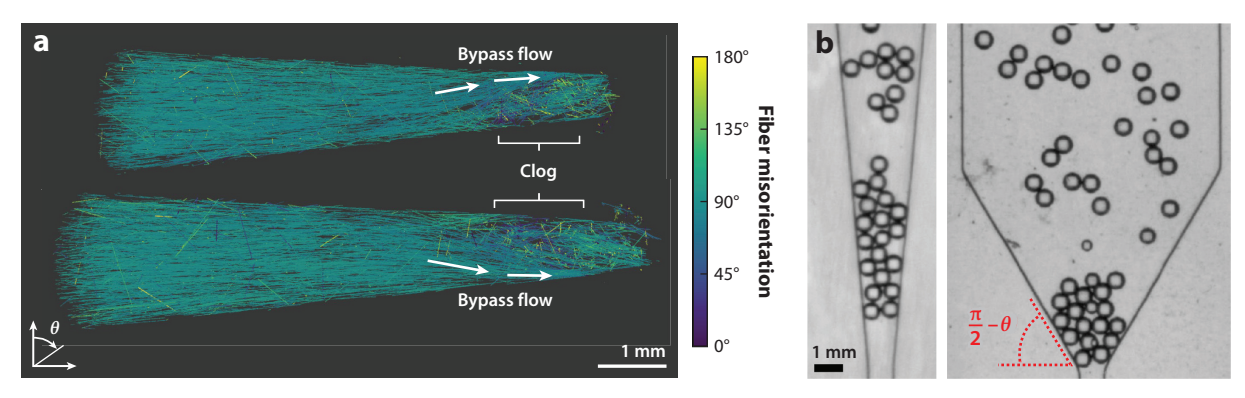


Figure 4

(a) 3D rendering of fiber orientation in a clogged nozzle used to dispense a fiber-reinforced ink composed of 5% SiC in an epoxy resin. Views are rotated approximately 45° around the nozzle axis. The color bar indicates the orientation of the fiber. Image provided by Brendan Croom. (b) Decreasing the angle θ of the nozzle delays the clogging by bridging for spherical particles, here shown in quasi-bidimensional systems. Panel reproduced from Vani et al. (2024) (CC BY 4.0).

as fibers (Hafez et al. 2021, Villalba et al. 2023). In particular, some DIW processes exhibit fiber bridging and entanglement. Croom et al. (2021) used in situ X-ray radiography and ex-situ X-ray computed tomography to probe the mechanisms behind nozzle clogging in the DIW printing of fiber-filled polymer inks (Figure 4a). These experiments revealed that, although fibers tend to align with the flow streamlines inside the nozzle, misaligned fibers can form log jams near the nozzle tip. Indeed, any perturbation can cause a fiber to rotate or bend, making contact with the nozzle walls. Once a few fibers misalign, they form a fibrous mat or bridge that traps others. This process often starts stochastically; e.g., a slight fluctuation causes one fiber to tumble, which then starts blocking others, eventually leading to a clog. Once a clog forms, the flow can either completely stop or force its way through a small channel, resulting in an unstable, pulsating extrusion. Fiber clogging is particularly important when printing inks with high fiber volume fractions. There is often a trade-off between adding fibers to enhance mechanical properties and the printability limit due to clogging. Longer fibers and higher volume fractions increase the likelihood of these clogs. The fluid mechanics here involves the interplay of flow-induced fiber orientation and confinement. High shear tends to align fibers with the flow, which is good for preventing clogs, but regions of recirculation or sudden contraction can disrupt alignment and lead to a clog (Villalba et al. 2023, Bräsel et al. 2024).

Clogging by aggregation, sometimes described as wall adhesion or fouling, is a gradual mechanism in which particles deposit and accumulate on the nozzle walls, progressively narrowing the flow channel (Wyss et al. 2006). Unlike bridging and sieving, aggregation clogs grow over time as particle–particle or particle–wall adhesion causes a fouling layer to develop. This is akin to colloidal deposition due to van der Waals forces, electrostatic attraction, or polymer bridging (Dersoir et al. 2015) in microfluidics. Aggregation is sensitive to surface chemistry and flow conditions. The constriction shrinks as the aggregate builds, eventually leading to a clog even if the particles are much smaller than the original nozzle size. The deposition of particles on the nozzle walls leads to an increase in extrusion pressure (for flow rate–driven flow) or a decrease in flow rate (for pressure-driven flow).

3.2.2. Influence of density mismatch and the rheology of the interstitial fluid. For suspensions used in DIW, it is rare that the particles are neutrally buoyant in the carrier fluid. Most DIW inks utilize water, polymer resins, alcohols, or other solvents as the carrier fluid, and

ceramic, carbon, and glass fibers are denser than the typical carrier fluids, while polymer and glass microballoons are generally less dense. In each case, DIW inks are susceptible to sedimentation (or creaming, where buoyant particles float to the top of the suspension) over time. If printing times are long relative to the characteristic sedimentation time of the particles, inks can separate within the material reservoir or nozzle. This leads to local regions of dilute and concentrated particles, which disrupt flow consistency and can cause clogging. In practice, most DIW inks are designed to have a yield stress in the quiescent state, minimizing the risk of sedimentation. However, low-viscosity inks may require agitation or recirculation to maintain homogeneity and prevent clogging due to sedimentation. Notable exceptions to this include bio-based inks for bio-printing and polymer/polymer composites, where cells, in the former case, or polymer particles, in the latter case, have a similar density to that of the carrier fluid.

Clogging by particles dispersed in non-Newtonian fluids, such as yield-stress fluids, has been barely considered in the fluid mechanics community. Yet, in addition to the role of the particles, if the pressure in the nozzle drops below the yield stress, the material can solidify in place, effectively forming a plug. In a yield-stress ink, flow cessation often leads to a permanent gel structure remaining in the nozzle. When attempting to resume, the pressure may initially be insufficient to break this gel, resulting in a clog. On the other hand, high extrusion pressures can cause particles to form a tightly packed configuration at the nozzle. Thus, there is a window of optimal pressure: If it is too low, the suspension will not restart (clogging by solidification), and if it is too high, it may induce a jam via particle jamming. Curing or setting reactions are extreme cases. If the ink begins to harden inside the nozzle due to heat, premature UV exposure, or simply time, it will result in a hardened clog. Overall, the role of complex rheologies, as used in DIW, in clogging remains to be explored.

3.2.3. Potential mitigation strategies for clogging. Because clogging is a critical issue in many applications, different strategies have been considered to mitigate these mechanisms. The optimization of the geometry can reduce clogging, as tapered nozzles have been shown to delay clogging by bridging for suspensions of spherical particles, as illustrated in **Figure 4b** (Vani et al. 2024). Additionally, matching the nozzle size to the particle size is crucial; typically using a nozzle diameter at least of order 10 times larger than the particle diameter is required. However, simply using an oversized nozzle can sacrifice print resolution, so optimized designs are needed to balance printability and clog resistance. Nozzle surface treatments can also help to prevent clogging by aggregation.

Although much less considered in fundamental fluid mechanics studies, optimizing the rheology and composition of the ink can help with clogging. For instance, using appropriate dispersants can prevent particle aggregation, and tuning viscosity and yield stress can help particles remain suspended. For fiber-filled inks, controlling the fiber aspect ratio and flexibility can reduce the chance of fiber bridging, as can tailoring the viscosity of the carrier fluid. For example, in a numerical study of short carbon fibers in nylon, Zhang et al. (2021) showed that lowering the viscosity of the interstitial fluid helped fibers align with the flow and eliminated many clogs. Conversely, Hmeidat et al. (2021) studied epoxy resin loaded with short carbon fibers and observed less frequent clogging and more consistent printing after increasing the viscosity of the epoxy through the addition of nanoclay. Clearly, more work is needed in this area. Particle size distribution is also important, but its role in the clogging of suspensions remains unclear, although it has been highlighted in the DIW community (Delarue et al. 2024, Hossain & Akhtar 2024).

Active methods can also prevent or delay clogging. For instance, pulsatile flow has been shown to delay clogging by aggregation (Dincau et al. 2020, 2022). Since vibrations are effective at delaying clogging by bridging in granular materials (Lozano et al. 2012), implementing vibration or ultrasound at the nozzle can also be an effective way to delay clogging.



3.2.4. Self-filtration. Distinct from the nozzle clogging mechanisms, dense suspensions can exhibit self-filtration, a mechanism by which the volume fraction upstream of the nozzle increases over time because the volume fraction of the suspension that escapes through the nozzle is slightly lower than the volume fraction in the reservoir (Haw 2004, Kulkarni et al. 2010). The consequences for DIW can be significant. The resulting increase in the local particle volume fraction increases the clogging probability. Even if the nozzle does not clog completely, self-filtration can lead to the extrusion of an ink with a lower-than-intended particle volume fraction, altering the composition of the filament. Self-filtration does not necessarily require large or specially shaped particles and can happen simply because of high volume fractions of particles. However, the influence of the nozzle geometry, volume fraction, particle shape, and fluid rheology on this process remains largely unexplored and deserves further study.

3.2.5. Particle migration. Suspension flows in confined geometries often exhibit shear-induced particle migration, which can lead to nonuniform particle distributions across the cross section of the nozzle. Particles tend to migrate from high-shear regions to low-shear regions (Leighton & Acrivos 1987, Frank et al. 2003). In a typical Newtonian pipe flow, this means particles drift away from the walls toward the centerline, where shear rates are lower. This phenomenon can create a core of concentrated particles along the flow axis. In viscoelastic fluids, additional migration effects can occur where normal stresses push particles toward the centerline or toward the walls, depending on the fluid rheology (see, e.g., D'Avino et al. 2017). In DIW, shear-induced migration may contribute to nozzle clogging by focusing particles in certain regions of the nozzle. In addition, even if a clog does not form, migration can still cause inhomogeneous filament compositions with a higher concentration of particles in the filament's core. This has been observed as a radial gradient in printed filaments for some inks. From a practical standpoint, controlling flow rates and nozzle length can modulate migration. Some DIW systems also introduce active mechanisms, such as acoustic focusing, to control the migration of the particles (Friedrich et al. 2017).

3.2.6. Fluid mechanics considerations for clogging in direct-ink writing. Direct numerical simulations, for instance with a coupled CFD-discrete element method approach, can provide insight into flow profiles and particle trajectories within confined systems and constrictions or into low-shear regions where aggregation might occur (Mondal et al. 2016, Kanarska et al. 2019). Such models could also incorporate the coupling between particles and more complex rheology (Li et al. 2015, Chaparian et al. 2020). However, simulation complexity grows rapidly with the number of particles and the rheology of the fluid, restricting the direct application of these models to relatively small-scale or simplified scenarios. Experimentally, the challenge is to visualize clogging. Researchers often employ transparent channels to observe clog formation in real time. Such experiments with model materials (e.g., spherical particles, fibers) in Newtonian solvents have revealed bridging dynamics and critical parameters affecting clogging, such as particle volume fraction and roughness. When direct observation is impractical (as in an opaque channel), clogging detection can rely on pressure and flow monitoring (Kopatz et al. 2024), as abrupt changes indicate incipient arches or flow obstructions. Overall, most fluid mechanics studies devoted to clogging have considered simple geometry, mainly Newtonian fluids, and spherical particles. Advances in our understanding of clogging will require considering more complex systems and geometries, such as 3D systems, and particles of complex shapes, such as fibers.

4. FORMATION, STABILITY, AND DEPOSITION OF FILAMENTS

Upon exiting the nozzle, the extruded fluid transitions into a free-surface flow, typically as a slender cylindrical filament moving relative to the environment, and is deposited on a substrate. Though

transient and sometimes overlooked, this intermediate phase influences the quality of the filament deposited and the printed geometry. While fluid mechanics studies have extensively characterized the formation of filaments and droplets in Newtonian homogeneous fluids, DIW printing introduces additional complexity, as it involves non-Newtonian fluids that may contain particles. These systems present unique fluid mechanical challenges that have been less explored than those involving Newtonian fluids.

4.1. Filament Formation and Die Swell

Due to the large viscosity of the ink, when a viscous fluid is extruded from a nozzle, the capillary number Ca is often large so that surface tension plays a comparatively minor role during extrusion but becomes important once the filament is formed and free. The initial filament diameter is thus usually set by rheology rather than capillarity. In particular, inks used in DIW often emerge with a diameter larger than the nozzle, a phenomenon known as die swell (Tang et al. 2020). Die swell occurs because fluid elements within the nozzle store elastic energy as polymer chains are stretched or oriented under shear. Upon exiting the nozzle, the relaxation of stored normal stresses (first normal stress difference N_1) allows partial elastic recoil, causing the filament to widen (De Rosa et al. 2023). This characteristic behavior, documented in the polymer processing literature (e.g., Tanner 1970, Pettas et al. 2015), is governed by fluid rheology and flow history.

The die-swell ratio α is defined as the ratio of the diameter of the filament and the nozzle diameter, $\alpha = D_{\text{lig}}/D$, and it increases with fluid elasticity, often quantified by the Weissenberg number $Wi = \lambda U/D$. In Newtonian cases, the swell ratio remains close to unity, exhibiting minimal expansion beyond minor pressure drop effects, as these materials lack the normal stress-driven recovery mechanism. In contrast, polymeric fluids can display substantially larger swell ratios. Tanner's law empirically states that the swell ratio $\alpha = D_{\text{lig}}/D$ is related to the first normal stress difference N_1 (Tanner 1970). Yield-stress fluids occupy an intermediate position. If the stress falls below the yield stress upon exit, expansion is constrained. In practice, yield-stress fluids often maintain nearly plug flow profiles upon exiting the die, occasionally exhibiting a slight contraction in the absence of elastic stresses. For shear-thinning and weakly elastic fluids, the steep viscosity gradient inside the nozzle flattens the velocity profile and limits velocity redistribution at the exit. As a result, the die-swell ratio increases monotonically with the flow index n (Mitsoulis et al. 1984).

In practice, excessive die swell is undesirable for print fidelity, as it means the deposited filament will be thicker than intended. Different strategies can help limit die swell, such as using lower elasticity inks or tapering nozzle geometries. Although die swell has been extensively studied in other contexts, different questions are raised by DIW inks, such as, for instance, the influence of particles dispersed in the fluid on the die swell (Mezi et al. 2019).

4.2. Stability of the Filament and Heterogeneous Fluids

Once the filament is formed and extruded, its thinning and stability primarily result from capillary and viscous forces. For a filament of Newtonian fluid of radius R, the classic Rayleigh–Plateau instability predicts that perturbations with wavelength $\lambda > 2\pi R$ are linearly unstable to axial perturbations (Eggers & Villermaux 2008). If the filament is sufficiently long, this condition results in the breakup of the filament into droplets. However, viscous effects extend the capillary breakup time while simultaneously stabilizing short-wavelength perturbations. The Ohnesorge number $Ob = \eta/\sqrt{\rho\gamma R}$ captures this balance; when $Ob \gg 1$, the filament thins slowly, whereas $Ob \ll 1$ promotes rapid pinch-off.

The rheology of the ink strongly influences the stability of the filament. In particular, viscoelastic fluids resist necking through extensional stresses so that a filament can persist for durations



exceeding a Newtonian thread by multiple orders of magnitude (Dinic & Sharma 2019, Rajesh et al. 2022). For a Deborah number $De \gg 1$ (indicating long relaxation times or rapid capillary dynamics), the filament enters an extended elastic stretching regime. When $De \ll 1$, elastic effects dissipate too rapidly to impede instability progression, resulting in breakup dynamics resembling Newtonian behavior. Polymer solutions can also exhibit a distinctive beads-on-a-string instability (Clasen et al. 2006, Bhat et al. 2010). Viscoplastic filaments introduce yet another stability mechanism, as a yield stress τ_Y can prevent pinch-off below a critical thread radius. Essentially, surface tension must generate sufficient stress of order γ/R to overcome τ_Y . This relationship defines a characteristic length scale $R_y \sim \gamma/\tau_Y$. When $R \gtrsim R_y$, capillary pinching becomes arrested by the finite strength of the material, causing the filament to exhibit solid-like behavior capable of self-supporting its weight without breaking. Experimental investigations with yield-stress fluids (e.g., Carbopol or clay suspensions) confirm that filaments below a critical diameter threshold resist further necking, instead forming stable cylindrical columns that either thin slowly via creep mechanisms or maintain dimensional stability indefinitely (Geffrault et al. 2023).

From a practical perspective, the key dimensionless parameters governing filament stability are the capillary number $Ca = \eta U/\gamma$ (the ratio of viscous to surface tension forces for axial flow speed U), De or Wi for elasticity, and the yield number $Y = \tau_Y R/\gamma$. Stable filaments require some combination of high Ca or Ob (to damp capillary waves), high De (to stress-harden the filament), or high Y (to resist deformation). When these conditions remain unsatisfied, the filament may rapidly develop undulations before breaking into droplets.

A challenge arises when particles are dispersed in the ink. Indeed, the presence of particles dispersed in the fluid can induce significant shear-thinning or yield-stress behaviors and can cause substantial deviations from Newtonian scaling relationships during filament formation. Different studies have shown that the presence of non-Brownian particles dispersed in a liquid also accelerates the pinch-off of liquid filaments (Furbank & Morris 2004, Château & Lhuissier 2019, Thiévenaz & Sauret 2021, Thiévenaz et al. 2021). Local particle rearrangements dynamically alter effective rheology while generating fluctuating stress fields within thinning regions. A challenge when printing fine features is to estimate when a macroscopic rheological approach that treats the suspension as an effectively homogeneous fluid provides an adequate approximation. Indeed, as the filament thickness approaches the particle scale, the flow exhibits marked nonuniformities and potential pinch-off that bulk rheological measurements alone cannot capture (Château et al. 2018, Thiévenaz & Sauret 2022b). Whereas homogeneous liquids often follow universal thinning laws that yield smooth, symmetric necks, the presence of solid inclusions perturbs the pinch-off region. In turn, this may accelerate filament breakup or generate irregular satellite droplets. Fibers can undergo alignment under extensional flow conditions, altering effective extensional viscosity (Château et al. 2021), while deformable inclusions may stabilize or destabilize the thinning filament depending on specific material properties and flow conditions (e.g., Thiévenaz & Sauret 2022a).

4.3. Filament Deposition

During filament deposition, various instabilities can emerge when flow dynamics and translation motion are imperfectly synchronized. Critical parameters governing this process include the extrusion velocity $V_{\rm e}$ of the ink emerging from the nozzle of diameter D, the translational velocity of the nozzle V relative to the substrate, and the stand-off height H between the nozzle and the deposition surface. The extrusion velocity relates to the volumetric flow rate, $Q = \pi V_{\rm e} (\alpha D)^2/4$, where $\alpha \geq 1$ accounts for the complex rheological effects, including die swelling. These parameters define distinct processing regimes, rationalized through dimensionless printing parameters: the nondimensional nozzle velocity $V^* \equiv V/V_{\rm e}$ and nondimensional stand-off height $H^* \equiv H/(\alpha D)$.

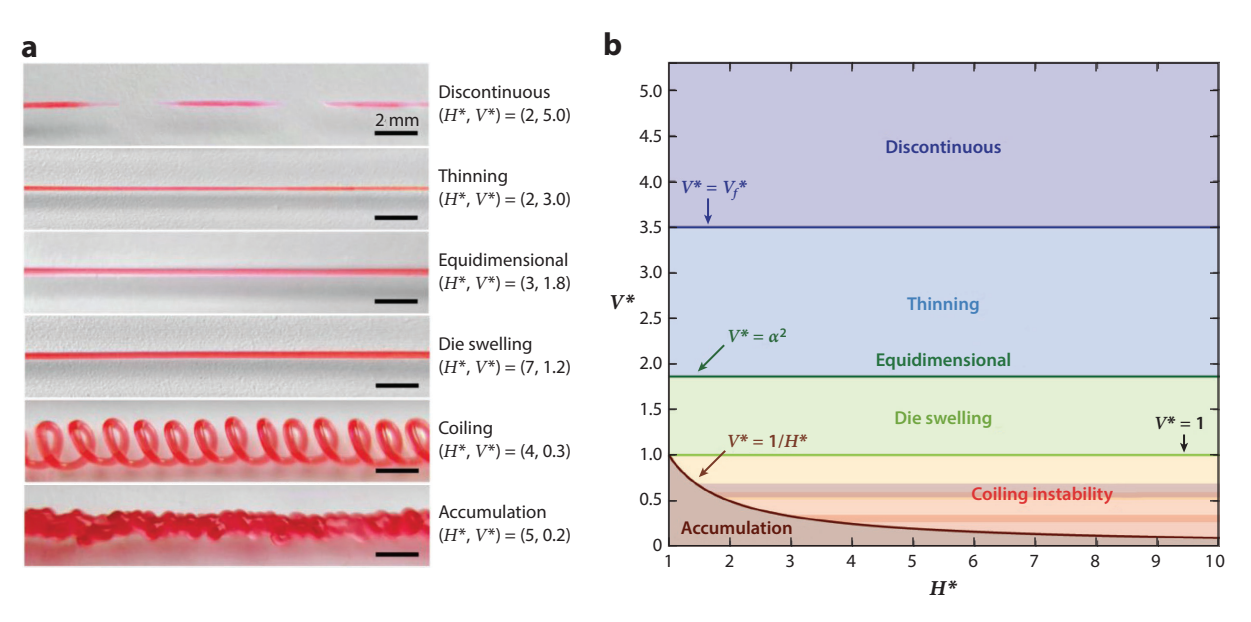


Figure 5

(a) Illustration of the stability of a filament of viscoelastic ink deposited when increasing the nondimensional nozzle speed V*. At low V^* , overextrusion causes accumulation or coiling; at intermediate V^* , a normal extrusion (straight filament) is observed; and high V^* leads to underextrusion, causing an intermittent filament. (b) Corresponding phase diagram for viscoelastic inks governed by nondimensional parameters (H^*, V^*). Figure adapted with permission from (Yuk & Zhao 2018).

Conventional printing processes typically maintain V^* and H^* close to unity, allowing filament deposition to occur with minimal deformation.

As Figure 5a illustrates, innovative approaches increasingly leverage controlled deformation and instabilities by operating outside this parameter space (Yuk & Zhao 2018). Overextrusion conditions ($V^* < 1$), where material delivery exceeds the nozzle translation speed, result in classic viscous buckling, coiling instabilities, and material accumulation (Chiu-Webster & Lister 2006). This phenomenon closely parallels the well-documented liquid rope coiling effect, where a viscous fluid thread spontaneously forms an organized loop pattern when accumulating on a surface (Ribe et al. 2012). At low substrate speeds, a falling viscous thread coils like a rope; at higher speeds, the thread can be stretched into meandering or looping patterns (Morris et al. 2008). These instabilities have been extensively characterized over recent decades following the pioneering work of Chiu-Webster & Lister (2006), who documented a rich variety of "fluid-mechanical sewing machine" patterns for a viscous thread on a moving belt (e.g., straight, meanders, loops, figure eights) depending on V^* and H^* (Brun et al. 2015). Such instabilities frequently manifest in DIW processes when nozzle translation and extrusion rates are mismatched. Indeed, strategic overextrusion in DIW protocols intentionally induces filament buckling or folding instead of linear deposition (Bandala et al. 2025). Conversely, under extrusion conditions ($V^* > 1$) with viscoelastic fluid, where material delivery falls below the nozzle translation speed, promote filament thinning during deposition, enabling the production of fine structural features (Yuk & Zhao 2018). However, when V* exceeds material-specific threshold values, discontinuous deposition patterns emerge (Geffrault et al. 2023, Coussot 2025). Phase diagrams across the (V^*, H^*) parameter space, as shown in Figure 5b for a given viscoelastic ink, highlight that transition boundaries between distinct regimes (as well as the detailed structure of coiling instabilities) depend on the ink's rheological properties.



5. FORM HOLDING

The critical phase following extrusion is filament deposition, where ink is strategically laid down to construct structures layer by layer. Print success requires maintaining filament stability, achieving precise material placement, and ensuring proper solidification. During deposition, the extruded material follows prescribed pathways as filaments or droplets, raising questions of free-surface flow dynamics, viscoplastic spreading, interfacial adhesion, and coalescence.

5.1. Spreading Dynamics and Shape Retention

After initial shape setting, filaments must solidify through mechanisms such as solvent evaporation, cooling, or curing to support subsequent layers. For solvent-based inks, commonly used in colloidal suspensions or bio-inks, solvent evaporation generates concentration gradients and capillary flows analogous to coffee-ring effects, which can potentially cause uneven particle distribution or filament cracking. UV-curable systems may experience shrinkage stresses during curing. Most DIW implementations avoid purely viscous liquid formulations since filament stability during solidification cannot be guaranteed. Instead, they rely on yield-stress materials that recover solid-like behavior shortly after deposition. Even with yield stress, some transient spreading occurs right after deposition. The layer may flatten over time if the ink does not recover its structure quickly or if the yield stress is insufficient (Figure 6a). Slow recovery may exacerbate postdeposition slumping.

When a fluid filament is deposited onto a substrate, it initially spreads radially due to capillary pressure, $\Delta P_{\text{cap}} \sim \gamma / b(t)$, where γ is the surface tension and b(t) is the filament height. While gravity dominates spreading in large-scale DIW processes, surface tension becomes the primary driver at smaller scales. The filament spreads until equilibrium is reached through either the balance of surface energy or the recovery of yield strength. Notably, a Newtonian fluid filament without solidification mechanisms will break into droplets if the contact lines retract. This fundamental limitation explains why DIW inks are engineered to recover or set rapidly once extrusion stresses dissipate (Tagliaferri et al. 2021).

Recent work by van der Kolk et al. (2023) examined single-line configurations of model yieldstress fluids. As shown in Figure 6b, filaments spread to a finite width until yield stress equilibrates with capillary forces, creating a stable pancake shape. The spreading velocity U(t) is governed by the balance

$$\gamma \frac{\partial b}{\partial r} \sim \tau_{\rm Y} + \eta_{\rm p} \, \dot{\gamma},$$
 3

where $\eta_{\rm p}$ is the plastic viscosity and the shear rate scales as $\dot{\gamma}U/b$. As can be expected, higher values of the yield stress τ_Y lead to less spreading, as illustrated in **Figure 6c**. For $\tau_Y \gg \eta_p \dot{\gamma}$ (i.e., at high Bingham numbers $Bn = \tau_Y D/\eta_p U$, the flow localizes near the contact line, forming a pseudoplug region where $\tau < \tau_Y$. The spreading stops when the capillary stress is balanced by the yield stress, leading to $R_f \sim \gamma / \tau_Y$, where R_f is the equilibrium filament radius. This balance defines the plastocapillary number $\mathcal J$ (see the sidebar titled Dimensionless Parameters). Experimental data for Carbopol gels confirm that $R_f/\mathcal{L} \propto \mathcal{J}$, with deviations occurring at high Bond numbers $B_\theta =$ $\rho g R_{\rm f}^2/\gamma \gg 1$, where gravitational effects become significant (van der Kolk et al. 2023). Unlike fully leveled Newtonian films, the plastocapillary spreading regime represents a fundamental concept in DIW, where filaments behave like viscoplastic droplets that stop spreading while maintaining raised profiles.

5.2. Coalescence and Layers Bonding

Effective bonding between deposited filaments and the substrate or previous layers is essential for the structural integrity of the printed structure. The physical state of each layer, whether fluid



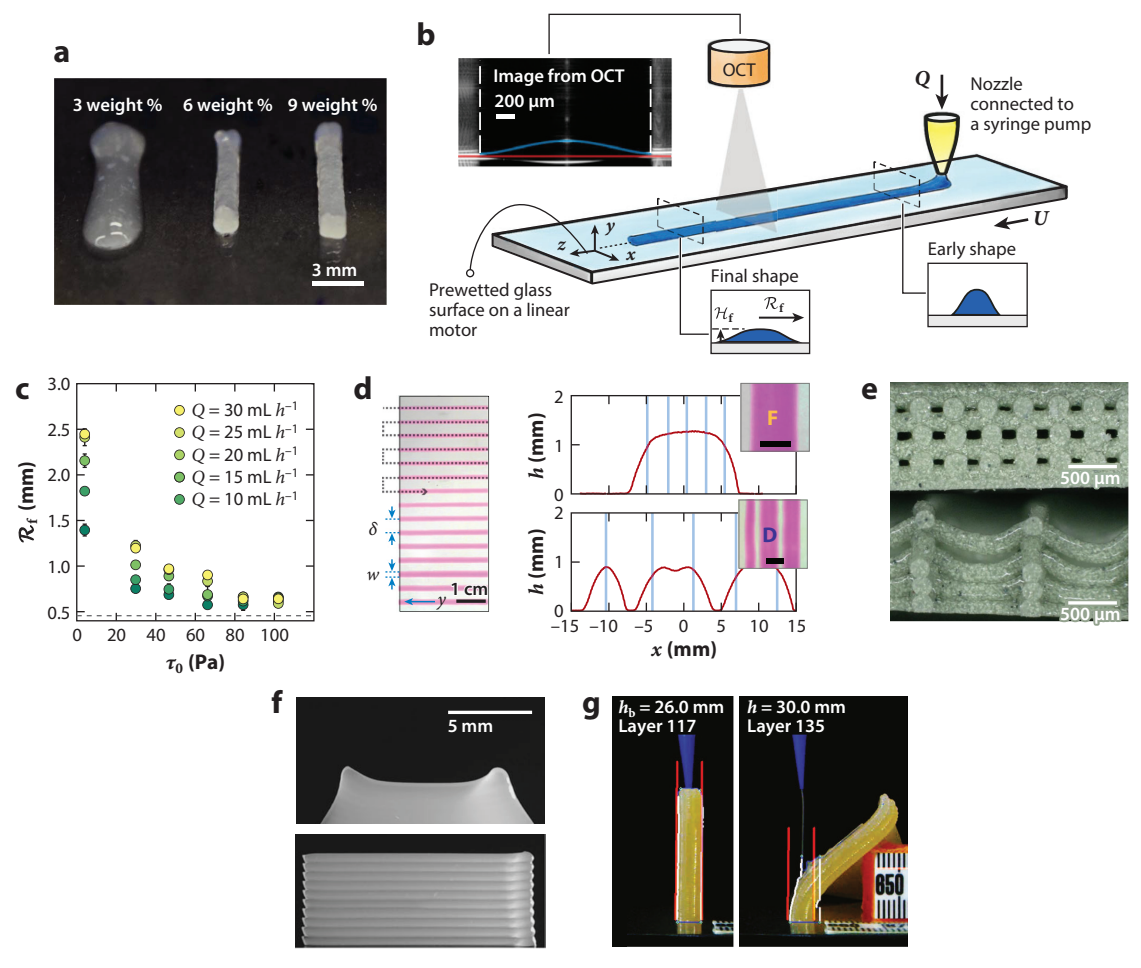


Figure 6

(a) Effect of yield stress on structure retention in printed filaments for different concentrations of functional living ink (Flink) leading to increasing yield stress: $\tau_Y \sim 20$ Pa, 150 Pa, and 360 Pa, from left to right. Panel adapted with permission from Schaffner et al. (2017). (b) Deposition of a filament of a yield-stress fluid on a moving prewetted substrate. The filament spreads on the surface until it reaches a final width. The inset shows an image from an optical coherence tomography (OCT) scanner, where blue and red lines highlight the interface of the filament and the substrate. (c) Final half-width of the printed line for different flow rates and yield-stress values. Panels b and c adapted from van der Kolk et al. (2023) (CC BY 4.0). (d) Serpentine pathway used to deposit a ligament of yield-stress fluids of controlled width w separated by a distance δ . Depending on the overlap ratio δ/w of the printed lines, different morphologies of the deposit are observed, such as continuous with a flat profile (F) for $\delta/w = 0.5$ or discontinuous (D) for $\delta/w = 1.1$. On the plots, the blue vertical lines indicate the position of the print path, and the red line is the profile. Panel adapted from Colanges et al. (2023) (CC BY 4.0). (e) Example of stable versus sagging ligaments for two different spacings. Panel adapted from Legett et al. (2022) (CC BY 4.0). (f) Example of slumping for 5-mm stacks of suspensions printed with a 500- μ m nozzle with yield stress $\tau_Y \sim 120$ Pa (top) and $\tau_Y \sim 350$ Pa (bottom). Panel adapted from M'barki et al. (2017) (CC BY 4.0). (g) Example of the buckling of a printed structure (wall) made of nanoclay ink. Panel adapted with permission from Romberg et al. (2021).

or solid, critically influences the quality of interfacial bonding. Wet-on-wet deposition involves printing new filaments onto still-fluid or uncured previous layers, enabling material coalescence and fusion. Conversely, wet-on-dry deposition occurs when the previous layer has solidified, often resulting in distinct interfaces or compromised adhesion (Fiske et al. 2018). Wet-on-wet printing can be understood through fluid mechanics as a coalescence phenomenon. When a fresh filament



is deposited onto a liquid or semiliquid layer, its interface behaves like merging droplets or viscous lenses (Eggers et al. 2024). The coalescence of Newtonian droplets or of a droplet with a film has been considered in various studies, but the case of viscoplastic fluids is more complex (Kern et al. 2022). Colanges et al. (2023) have shown that controlling the width and spacing of filaments of yield-stress fluids can lead to films with a smooth, continuous final profile, as shown in **Figure 6d**. If a new filament is deposited on a still-wet layer, the two may partially merge, which can be beneficial for bonding but may also cause additional spreading or sagging due to the liquid-liquid interface. For instance, Jalaal et al. (2021) examined yield-stress fluid droplets spreading on thin films of identical composition, providing an idealized model for layer-on-layer deposition dynamics.

5.3. Stability of Printed Structures

As 3D structures develop through filament stacking, the weight burden on lower filaments increases progressively. DIW-constructed structures may deform or collapse under their own weight if the constituent materials lack sufficient yield stress or solidification capacity to withstand accumulated stresses. Empirical studies reveal multiple stability failure mechanisms, with gap spanning, slumping, viscoelastic buckling, and plastic collapse being the most common.

5.3.1. Gap-spanning filament. When DIW filaments bridge gaps between supports, they inevitably sag under gravitational forces, adopting catenary shapes that may contact underlying layers or rupture (Smay et al. 2002, Ribeiro et al. 2017). In this mode, the deformation magnitude increases with the span length and decreases with the fluid yield stress (**Figure 6e**). While yield stress is crucial for preventing permanent plastic deformation, the elastic modulus of the ink provides the initial resistance to sagging. Therriault et al. (2007) introduced a filament collapse test measuring mid-span deflection, which correlates directly to yield stress and viscoelasticity. They observed that inks with a higher solid content, and thus higher yield stress and storage modulus G', produce filaments with significantly reduced sag angles, while low-viscosity formulations collapse readily. Fluids with insufficient yield stress exhibit catastrophic failure in span tests, either sagging until substrate contact occurs or breaking mid-span. Such failures delineate the printability limit for gap spanning, as an ink must have a minimum yield stress to hold its own weight. More recently, Saengow et al. (2025) demonstrated that optimal gap-spanning performance requires both sufficient yield stress to resist sagging and high extensibility to tolerate stretching without pinch-off.

For small deflections, one can model a spanning filament as a simply-supported beam of length L, weight per length $w = \rho Ag$ (with ρ being the density, A the cross-sectional area, and g gravity), and bending stiffness EI. The deflected shape y(x) satisfies the beam equation EI, y''''(x) = w. The classic solution gives a maximum deflection at mid-span of $\delta_{\max} = (5wL^4)/(384EI)$ for a uniformly loaded beam of length L. At first order, a stiffer filament or shorter span (large EI or small L) sags less. However, DIW filaments exhibit yield-stress and viscoelastic behaviors rather than ideal elastic responses. Before any yielding occurs, the filament will sag elastically under its own weight. The extent of this initial, recoverable deformation is governed by the storage modulus G'. If the self-weight of the filament induces stress beyond the yield stress τ_Y , the material will flow or plastically deform until stresses drop to τ_Y . By balancing the gravitational force against the yield resistance, the critical span L_c that a cylindrical filament of diameter d can self-support can be estimated as

$$\tau_{\rm Y} \sim \frac{\rho g A L_{\rm c}^2}{8I} = \frac{2\rho g L_{\rm c}^2}{d^2},\tag{4}$$

so that $L_c \sim [\tau_Y d^2/2\rho g]^{1/2}$. This simple scaling captures the intuitive trends observed in experiments: stronger, thicker filaments support longer spans, whereas heavy or weak (low τ_Y) filaments collapse at shorter lengths. More rigorous theoretical treatments of hanging viscoplastic filaments have been developed using slender-body and catenary theory. For instance, Kamrin & Mahadevan (2012) derived nonlinear equations for filaments of arbitrary rheology (Maxwell fluids, Bingham plastics, etc.) undergoing sagging and showed that a yield-stress filament will sag over time and then stop once the stress falls to $\tau_{\rm Y}$. However, this model of plastic failure does not account for the initial elastic sagging, which can also be a limiting factor in print quality. A high extensional viscosity, often correlated with the material's elasticity, can also play a role in preventing the filament from thinning and rupturing under its own weight.

Surface tension minimizes curvature and can partially counteract sagging but may simultaneously induce filament pinch-off. At high plastocapillary numbers \mathcal{J} (high yield stress relative to surface tension), filaments resist necking and exhibit solid-like behavior; at lower values, filaments may thin or rupture through capillary pinch-off. For typical DIW filaments (0.1-1 mm in diameter) over a large enough gap, gravitational effects generally predominate, though capillarity may introduce subtle modifications.

5.3.2. Slumping. Similar to individual filaments, columns created from stacked filaments can bulge and slump under their own weight when mechanical strength is insufficient (Figure 6f). Even initially stable structures may experience gradual creep if the constituent fluid undergoes slow structural recovery. Thixotropic inks that require a long time to rebuild stiffness may exhibit a time-dependent slump, where layers slowly flatten as the underlying material yields.

The maximum height H of a self-supporting column of cross-sectional area A made of a viscoplastic material of yield stress $\tau_{\rm Y}$ can be estimated by considering that the compressive stress at the base due to the weight of the column, ρgH , should not exceed the yield stress of the material τ_Y (Liu et al. 2016, Romberg et al. 2021). Thus, $H_c \approx \tau_Y/(\rho g)$ is the approximate critical height where a yield-stress fluid column begins yielding under self-weight—analogous to measurements in classical slumping tests (Staron et al. 2013). In practice, finite yield-stress fluids initiate slumping once a threshold layer count or height is reached. Indeed, beyond this threshold, as additional material is deposited, the lower layers yield and flow laterally, enlarging the effective cross-sectional area $A_{\rm eff}$. This lateral spreading reduces the self-weight stress to $\rho g H_{\rm new}$, and once that stress drops below the yield stress τ_Y , the deformation stops.

5.3.3. Viscoelastic buckling and plastic collapse. When an ink possesses sufficient yield strength to suppress slumping after deposition, tall slender structures may fail through buckling rather than uniform slumping. The buckling mechanics of near-vertical viscoplastic columns have been theoretically analyzed by Balmforth & Hewitt (2013), while self-weight-induced buckling of tall elastic columns was studied for many decades. Recently, Romberg et al. (2021) investigated the structural stability of printed thin walls, demonstrating that buckling instabilities can be accurately predicted using simple elastic buckling models under self-weight considerations, provided the recovered storage modulus after shear excursion was used to calculate the critical height for buckling (Figure 6g). Consequently, even perfectly elastic materials have maximum self-supporting height before lateral buckling occurs in slender configurations. Furthermore, Romberg et al. (2022a) found that even small deviations (~5°) from vertical caused the failure mode to transition from elastic buckling to plastic collapse, dictated by the yield stress of the ink through the fully plastic moment of the wall. Finally, the DIW process introduces additional perturbations, such as machine vibrations and forces transmitted from the nozzle to the printed object, that can trigger instabilities or potentially slow or prevent full recovery of the storage modulus and yield stress.



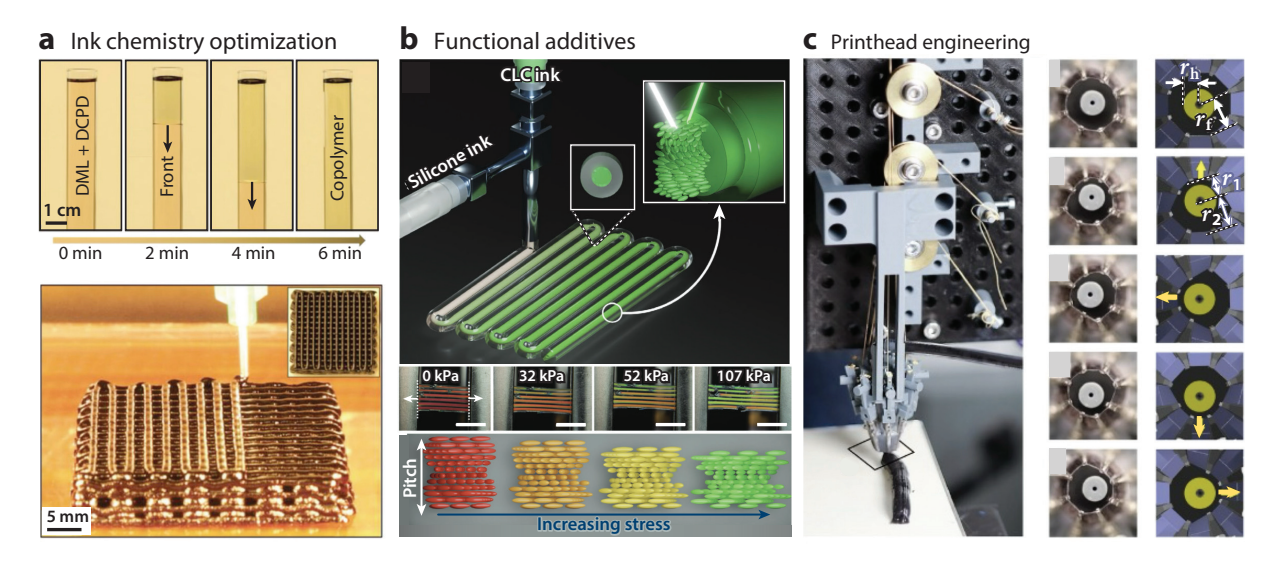


Figure 7

Emerging areas of innovation in direct-ink writing printing center on (*a*) optimizing the ink chemistry to enhance curing, (*b*) including additives to impart additional functionality in a printed component, and (*c*) developing active nozzles that enable additional layers of control over a printed line. Abbreviations: CLC, cholesteric liquid crystal; DCPD, dicyclopentadiene; DML, DCPD-modified linseed oil. Panel *a* adapted with permission from Ziaee et al. (2023); copyright 2023 American Chemical Society. Panel *b* adapted from Ng et al. (2025) (CC BY 4.0). Panel *c* adapted with permission from Kang & Mueller (2025).

6. CONCLUSION: OUTLOOK, CHALLENGES, AND OPEN QUESTIONS

DIW enables the fabrication of 3D structures through the extrusion of rheologically complex fluids, with success dependent on precise control of the fluid mechanics processes involved. Within the nozzle, shear-thinning, viscoelastic, and yield-stress behaviors govern extrudability, while particle-laden inks may trigger clogging. Postextrusion, extensional flows form filaments whose integrity depends on the balance between capillary forces, gravity, and rheological properties. On the substrate, controlled spreading and microstructural recovery ensure shape retention, whereas insufficient yield stress leads to structural slumping. Improving DIW processes requires developing fundamental models based on fluid mechanics principles, bridging rheological measurements, experimental approaches, dimensionless scaling analyses, and computational models to predict outcomes and optimize ink formulations, nozzle geometries, and printing protocols. Such knowledge will then enable the development and improvement of new DIW approaches (**Figure 7**).

While still peripheral to most DIW research efforts, a growing body of work demonstrates that the performance envelope of DIW can be significantly expanded when physicochemical transformations are programmed to occur during or immediately after extrusion. Strategies range from latent, heat-triggered (McKenzie & Koerner 2020), or photo-initiated chemistries (Yirmibesoglu et al. 2021) that remain quiescent under high shear but solidify within seconds after deposition to exothermic frontal ring-opening metathesis polymerization (FROMP) that converts centimeter-scale features into stiff thermosets via self-propagating reaction fronts (Aw et al. 2022). Inks containing blocked isocyanates (Wang et al. 2024), microencapsulated cross-linkers (Jiang et al. 2023), or dual-cure epoxies (Kopatz et al. 2021) have likewise enabled the printing of elastomers, structural composites, and even ceramic precursors that were previously considered unprintable, while inline mixers (Teves et al. 2024) or concentric-nozzle geometries (Brown et al. 2025) allow two-part systems to be combined only at the point of deposition, eliminating pot-life

constraints. Such advances underscore the need for fluid mechanics models that embed reactionrate expressions into continuum descriptions of shear-thinning and yield-stress behavior so that flow stability, filament coalescence, and postdeposition solidification can be predicted simultaneously. Complementary efforts seek to harness external fields (e.g., magnetic, electric, acoustic) with fluid mechanics to manipulate ink microstructure or trigger solidification without altering the underlying chemistry (Johnson et al. 2021). As these stimuli act at a distance and can be modulated on subsecond timescales, they provide additional forms of control over microstructure and material properties.

Taken together, stimulus-responsive kinetics, reactive ink chemistries, and field-directed assembly shift DIW from a purely kinematic patterning strategy to a platform for spatiotemporal materials synthesis. The fluid mechanics theory and models reviewed herein therefore do more than describe flow through a nozzle: They offer a predictive framework for synchronizing shear histories, residence times, chemical conversion, and field interactions so that solidification by design can be rationally implemented, whether via FROMP (Aw et al. 2022, Kim et al. 2025), in situ UV curing (Kopatz et al. 2021), or print-on-demand mixing of reactive components (Uitz et al. 2021, Romberg et al. 2022b). By explicitly coupling viscoelastic flow models with reaction-diffusion and field-interaction terms, next-generation simulations will inform the inverse design of inks, nozzle geometries, and tool paths, accelerating the creation of DIW structures whose mechanical, electrical, and biological performance is encoded from the nozzle to the final part.

SUMMARY POINTS

- Successful direct-ink writing printing requires a balance of key rheological properties.
 Shear-thinning behavior enables extrudability under moderate pressures. Yield stress provides shape retention to prevent slumping after deposition. Viscoelasticity influences the stability of the filament, die-swell effects, gap spanning by elastic recoil, and interlayer adhesion.
- Clogging is a key issue for particle-laden inks in nozzles. Recent efforts clarify how bridging, sieving, and aggregation act collectively in nozzles, with phenomena like fiber orientation and self-filtration adding further complexity in dense or anisotropic suspensions.
- 3. Filament formation and extensional dynamics are important for print resolution. The transition from a confined flow in a nozzle to free-surface flow promotes die swell and potential necking instabilities. Non-Newtonian effects, including extensional thickening and viscoplastic resistance, significantly modify filament stability compared with classical Rayleigh–Plateau behavior.
- 4. Flow stability is highly sensitive to nozzle geometry and process parameters. Sudden contractions increase the pressure drop and induce undesirable recirculation, whereas tapered geometries can mitigate clogging. Dimensionless criteria help create printability maps that guide the selection of these parameters for different complex fluids.
- 5. Deposition onto the substrate involves spreading and coalescence and requires mechanical robustness. Capillary forces, gravitational loading, and rheological recovery dictate the final filament profiles. Yield stress and viscoelastic phenomena determine whether gap-spanning filaments sag or buckle, while stacked columns may slump if the self-weight exceeds the critical yield strength.

FUTURE ISSUES

- The rheology and printability of complex suspensions remain a key challenge, requiring improved modeling frameworks to describe suspensions of polydisperse or complex-shaped particles in non-Newtonian carrier fluids. Of particular importance are extensional flow regimes to capture thinning dynamics and potential pinch-off singularities, which are only partially understood.
- 2. Clogging, particularly its modeling and prevention, requires further research as our current understanding, especially for complex fluids, is mainly empirical. There is a need to develop guidelines for particles of complex shapes in different geometries dispersed in non-Newtonian interstitial fluids. Vibration, ultrasonic agitation, and pulsatile flows can mitigate clogging in granular or fibrous suspensions, but the underlying fluid mechanics has not been systematically characterized.
- 3. The free-surface flow of heterogeneous fluids poses a challenge as complex suspensions transition from confined to free-surface flow, continuum approaches may fail when the extrusion diameter approaches the particle scale or when large aggregates form. Identifying dimensionless criteria for when discrete, particle-level physics must be accounted for will improve predictions of filament stability, breakup, and shape fidelity.
- 4. Exploiting deposition instabilities for advanced geometries presents a new design capability, moving beyond the traditional view of coiling or meandering of extruded filaments as a defect. However, harnessing these instabilities with carefully tuned fluid rheology and substrate motion may enable novel multiscale architectures. Quantifying their onset criteria would expand our design capabilities.
- 5. Although we did not discuss the solidification of the filament in this review, its deposition involves both fluid deformation and emergent solidification (via cross-linking, cooling, or evaporation). Current models typically treat these independently. More integrated numerical frameworks that simultaneously solve non-Newtonian flow and phase-change kinetics could help direct ink-writing processes.

DISCLOSURE STATEMENT

The authors are not aware of any affiliations, memberships, funding, or financial holdings that might be perceived as affecting the objectivity of this review.

ACKNOWLEDGMENTS

We thank Randy Ewoldt and Matthew Begley for their valuable input and comments on the manuscript. This work was partially supported by National Science Foundation (NSF) Faculty Early Career Development (CAREER) Program awards CBET 1944844 (A.S.) and CMMI 2240170 (T.R.R.), ACS PRF 69147-ND9 (A.S.), NSF grant OIA 2229784 (T.R.R.), and the Air Force Office of Scientific Research under grant W911NF-23-1-0162 (T.R.R.). Research reported in this publication was supported by the National Institute of General Medical Sciences of the National Institutes of Health under award number P20GM113134-06A1 (T.R.R.). B.G.C. acknowledges support from the Department of Energy's Kansas City National Security Campus, operated by Honeywell Federal Manufacturing & Technologies, LLC, under contract DE-NA0002839. The views and conclusions contained in this document are those of the authors

and should not be interpreted as representing the official policies, either expressed or implied, of the Air Force Office of Scientific Research or the US Government.

LITERATURE CITED

- Agrawal R, Garca-Tuñón E. 2024. Interplay between yielding, 'recovery', and strength of yield stress fluids for direct ink writing: new insights from oscillatory rheology. *Soft Matter* 20(37):7429–47
- Aguayo J, Tamaddon-Jahromi H, Webster M. 2008. Excess pressure-drop estimation in contraction and expansion flows for constant shear-viscosity, extension strain-hardening fluids. *J. Non-Newton. Fluid Mech.* 153(2–3):157–76
- Alves MA, Oliveira PJ, Pinho FT. 2004. On the effect of contraction ratio in viscoelastic flow through abrupt contractions. J. Non-Newton. Fluid Mech. 122(1-3):117-30
- Aw JE, Zhang X, Nelson AZ, Dean LM, Yourdkhani M, et al. 2022. Self-regulative direct ink writing of frontally polymerizing thermoset polymers. *Adv. Mater. Technol.* 7(9):2200230
- Balmforth NJ, Frigaard IA, Ovarlez G. 2014. Yielding to stress: recent developments in viscoplastic fluid mechanics. Annu. Rev. Fluid Mech. 46:121–46
- Balmforth NJ, Hewitt IJ. 2013. Viscoplastic sheets and threads. J. Non-Newton. Fluid Mech. 193:28-42
- Baloch A, Townsend P, Webster M. 1996. On vortex development in viscoelastic expansion and contraction flows. J. Non-Newton. Fluid Mech. 65(2-3):133-49
- Bandala E, Raymond L, Mitchell K, Rubbi F, Thella J, et al. 2025. Distance-controlled direct ink writing of titanium alloy with enhanced shape diversity and controllable porosity. NPJ Adv. Manuf. 2(1):4
- Bhat PP, Appathurai S, Harris MT, Pasquali M, McKinley GH, Basaran OA. 2010. Formation of beads-on-a-string structures during break-up of viscoelastic filaments. *Nat. Phys.* 6(8):625–31
- Blutinger JD, Cooper CC, Karthik S, Tsai A, Samarelli N, et al. 2023. The future of software-controlled cooking. NP7 Sci. Food 7(1):6
- Bonn D, Denn MM, Berthier L, Divoux T, Manneville S. 2017. Yield stress materials in soft condensed matter. *Rev. Mod. Phys.* 89(3):035005
- Bos F, Wolfs R, Ahmed Z, Salet T. 2016. Additive manufacturing of concrete in construction: potentials and challenges of 3D concrete printing. *Virtual Phys. Prototyp.* 11(3):209–25
- Bouslog S, Sidor A, Hagen R, Fowler M. 2021. 3D printing heat shields. Poster presented at the NASA JSC CIF Technology Show Case and Tech Port
- Boyko E, Stone HA. 2021. Flow rate–pressure drop relation for shear-thinning fluids in narrow channels: approximate solutions and comparison with experiments. *J. Fluid Mech.* 923:R5
- Bräsel B, Geiger M, Linkhorst J, Wessling M. 2024. Transport and clogging dynamics of flexible rods in pore constrictions. Soft Matter 20(34):6767–78
- Brown NC, Ames DC, Mueller J. 2025. Multimaterial extrusion 3D printing printheads. *Nat. Rev. Mater.* https://doi.org/10.1038/s41578-025-00809-y
- Brun PT, Audoly B, Ribe NM, Eaves TS, Lister JR. 2015. Liquid ropes: a geometrical model for thin viscous jet instabilities. *Phys. Rev. Lett.* 114(17):174501
- Buswell RA, Leal de Silva WR, Jones SZ, Dirrenberger J. 2018. 3D printing using concrete extrusion: a roadmap for research. *Cement Concrete Res.* 112:37–49
- Cesarano J. 1998. A review of robocasting technology. MRS Online Proc. Libr. 542:133
- Chan SS, Pennings RM, Edwards L, Franks GV. 2020. 3D printing of clay for decorative architectural applications: effect of solids volume fraction on rheology and printability. *Addit. Manuf.* 35:101335
- Chaparian E, Ardekani MN, Brandt L, Tammisola O. 2020. Particle migration in channel flow of an elastoviscoplastic fluid. J. Non-Newton. Fluid Mech. 284:104376
- Château J, Guazzelli É, Lhuissier H. 2018. Pinch-off of a viscous suspension thread. *J. Fluid Mech.* 852:178–98 Château J, Guazzelli É, Lhuissier H. 2021. Extensional viscosity and thinning of a fiber suspension thread. *Phys. Rev. Fluids* 6(4):044307
- Château J, Lhuissier H. 2019. Breakup of a particulate suspension jet. Phys. Rev. Fluids 4(1):012001
- Chiu-Webster S, Lister JR. 2006. The fall of a viscous thread onto a moving surface: a 'fluid-mechanical sewing machine.' J. Fluid Mech. 569:89–111

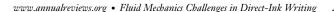


- Clasen C, Eggers J, Fontelos MA, Li J, McKinley GH. 2006. The beads-on-string structure of viscoelastic threads. J. Fluid Mech. 556:283–308
- Colanges S, Tourvieille J-N, Lidon P, Leng J. 2023. 2.5D printing of a yield-stress fluid. Sci. Rep. 13(1):5155
- Compton BG, Bui PP, Romberg SK, Kemp JW, Reed JL, et al. 2025. 3D-printed SiC-microfiber-reinforced polymer-derived ceramic with high strength at elevated temperature. J. Am. Ceram. Soc. 2025:e70143
- Compton BG, Hmeidat NS, Pack RC, Heres MF, Sangoro JR. 2018. Electrical and mechanical properties of 3D-printed graphene-reinforced epoxy. JOM 70:292–97
- Compton BG, Lewis JA. 2014. 3D-printing of lightweight cellular composites. Adv. Mater. 26(34):5930-35
- Coussot P. 2005. Rheometry of Pastes, Suspensions, and Granular Materials: Applications in Industry and Environment. Wiley
- Coussot P. 2025. Fifty shades of yield stress fluids: rheological challenges and engineering perspectives. *Rheol. Acta* 64:167–93
- Croom BP, Abbott A, Kemp JW, Rueschhoff L, Smieska L, et al. 2021. Mechanics of nozzle clogging during direct ink writing of fiber-reinforced composites. Addit. Manuf. 37:101701
- Culmone C, Smit G, Breedveld P. 2019. Additive manufacturing of medical instruments: a state-of-the-art review. *Addit. Manuf.* 27:461–73
- D'Avino G, Greco F, Maffettone PL. 2017. Particle migration due to viscoelasticity of the suspending liquid and its relevance in microfluidic devices. *Annu. Rev. Fluid Mech.* 49:341–60
- De Rosa S, Tammaro D, D'Avino G. 2023. Experimental and numerical investigation of the die swell in 3D printing processes. *Micromachines* 14(2):329
- De Smedt S, Attaianese B, Cardinaels R. 2025. Direct ink writing of particle-based multiphase materials: from rheology to functionality. *Curr. Opin. Colloid Interface Sci.* 75:101889
- Delarue AP, McAninch IM, Peterson AM, Hansen CJ. 2024. Increasing printable solid loading in digital light processing using a bimodal particle size distribution. 3D Print. Addit. Manuf. 11(5):e1819–28
- Delouche N, Schofield AB, Tabuteau H. 2020. Dynamics of progressive pore clogging by colloidal aggregates. Soft Matter 16(43):9899–907
- Derby B. 2010. Inkjet printing of functional and structural materials: fluid property requirements, feature stability, and resolution. *Annu. Rev. Mater. Res.* 40:395–414
- Dersoir B, de Saint Vincent MR, Abkarian M, Tabuteau H. 2015. Clogging of a single pore by colloidal particles. *Microfluid. Nanofluid.* 19(4):953–61
- Dincau B, Dressaire E, Sauret A. 2020. Pulsatile flow in microfluidic systems. Small 16(9):1904032
- Dincau B, Dressaire E, Sauret A. 2023. Clogging: the self-sabotage of suspensions. Phys. Today 76(2):24–30
- Dincau B, Tang C, Dressaire E, Sauret A. 2022. Clog mitigation in a microfluidic array via pulsatile flows. *Soft Matter* 18(9):1767–78
- Dinic J, Sharma V. 2019. Macromolecular relaxation, strain, and extensibility determine elastocapillary thinning and extensional viscosity of polymer solutions. PNAS 116(18):8766–74
- Dinkgreve M, Paredes J, Denn MM, Bonn D. 2016. On different ways of measuring "the" yield stress. J. Non-Newton. Fluid Mech. 238:233–41
- Dressaire E, Sauret A. 2017. Clogging of microfluidic systems. Soft Matter 13(1):37-48
- Duchêne C, Filipe V, Huille S, Lindner A. 2020. Clogging of microfluidic constrictions by monoclonal antibody aggregates: role of aggregate shape and deformability. *Soft Matter* 16(4):921–28
- Eggers J, Sprittles JE, Snoeijer JH. 2024. Coalescence dynamics. Annu. Rev. Fluid Mech. 57:61-87
- Eggers J, Villermaux E. 2008. Physics of liquid jets. Rep. Prog. Phys. 71(3):036601
- Ewoldt RH, Saengow C. 2022. Designing complex fluids. Annu. Rev. Fluid Mech. 54:413-41
- Férec J, Bertevas E, Khoo BC, Ausias G, Phan-Thien N. 2016. The effect of shear-thinning behaviour on rod orientation in filled fluids. 7. Fluid Mech. 798:350–70
- Fiske M, Edmunson JE, Weite E, Fikes JC, Johnston M, et al. 2018. The disruptive technology that is additive construction: system development lessons learned for terrestrial and planetary applications. In 2018 AIAA SPACE and Astronautics Forum and Exposition. AIAA
- Frank M, Anderson D, Weeks ER, Morris JF. 2003. Particle migration in pressure-driven flow of a Brownian suspension. *7. Fluid Mech.* 493:363–78
- Frazier WE. 2014. Metal additive manufacturing: a review. 7. Mater. Eng. Perform. 23:1917–28

- Friedrich L, Collino R, Ray T, Begley M. 2017. Acoustic control of microstructures during direct ink writing of two-phase materials. Sens. Actuators A Phys. 268:213-21
- Friedrich LM, Seppala JE. 2021. Simulated filament shapes in embedded 3D printing. Soft Matter 17(35):8027-
- Furbank RJ, Morris JF. 2004. An experimental study of particle effects on drop formation. Phys. Fluids 16(5):1777-90
- Garca-Tuñón E, Agrawal R, Ling B, Dennis DJ. 2023. Fourier-transform rheology and printability maps of complex fluids for three-dimensional printing. Phys. Fluids 35(1):017113
- Geffrault A, Bessaies-Bey H, Roussel N, Coussot P. 2023. Printing by yield stress fluid shaping. Addit. Manuf.
- Gibson I, Rosen D, Stucker B, Khorasani M. 2021. Additive Manufacturing Technologies. Springer. 3rd ed.
- Goldsztein GH, Santamarina JC. 2004. Suspension extraction through an opening before clogging. Appl. Phys. Lett. 85(19):4535-37
- Groll J, Boland T, Blunk T, Burdick J, Cho D, et al. 2016. Biofabrication: reappraising the definition of an evolving field. Biofabrication 8(1):013001
- Grosskopf AK, Truby RL, Kim H, Perazzo A, Lewis JA, Stone HA. 2018. Viscoplastic matrix materials for embedded 3D printing. ACS Appl. Mater. Interfaces 10(27):23353-61
- Guazzelli É, Pouliquen O. 2018. Rheology of dense granular suspensions. J. Fluid Mech. 852:P1
- Hafez A, Liu Q, Finkbeiner T, Alouhali RA, Moellendick TE, Santamarina JC. 2021. The effect of particle shape on discharge and clogging. Sci. Rep. 11:3309
- Haw M. 2004. Jamming, two-fluid behavior, and "self-filtration" in concentrated particulate suspensions. Phys. Rev. Lett. 92(18):185506
- Hinton TJ, Jallerat Q, Palchesko RN, Park JH, Grodzicki MS, et al. 2015. Three-dimensional printing of complex biological structures by freeform reversible embedding of suspended hydrogels. Sci. Adv. 1(9):e1500758
- Hmeidat NS, Elkins DS, Peter HR, Kumar V, Compton BG. 2021. Processing and mechanical characterization of short carbon fiber-reinforced epoxy composites for material extrusion additive manufacturing. Composites Part B Eng. 223:109122
- Ho M, Ramirez AB, Akbarnia N, Croiset E, Prince E, et al. 2025. Direct ink writing of conductive hydrogels. Adv. Funct. Mater. 35(22):2415507
- Hossain SS, Akhtar F. 2024. Effect of oxide nanoparticles in aqueous alumina inks for material extrusion additive manufacturing. 7. Eur. Ceram. Soc. 44(11):6668-76
- Hou Y, Baig MM, Lu J, Zhang H, Liu P, et al. 2024. Direct ink writing 3D printing of low-dimensional nanomaterials for micro-supercapacitors. Nanoscale 16(26):12380-96
- Hsu CP, Baysal HE, Wirenborn G, Mårtensson G, Wittberg LP, Isa L. 2021. Roughness-dependent clogging of particle suspensions flowing into a constriction. Soft Matter 17(31):7252-59
- Jalaal M, Stoeber B, Balmforth NJ. 2021. Spreading of viscoplastic droplets. J. Fluid Mech. 914:A21
- Jiang Y, Ng ELL, Han DX, Yan Y, Chan SY, et al. 2023. Self-healing polymeric materials and composites for additive manufacturing. Polymers 15(21):4206
- Johnson K, Melchert D, Gianola DS, Begley M, Ray TR. 2021. Recent progress in acoustic field-assisted 3D-printing of functional composite materials. MRS Adv. 6(25):636–43
- Kamrin K, Mahadevan L. 2012. Soft catenaries. 7. Fluid Mech. 691:165-77
- Kanarska Y, Duoss EB, Lewicki JP, Rodriguez JN, Wu A. 2019. Fiber motion in highly confined flows of carbon fiber and non-Newtonian polymer. J. Non-Newton. Fluid Mech. 265:41-52
- Kang SW, Mueller J. 2025. Adaptive core-shell 3D printing of hollow fiber actuators. Device 3(8):100799
- Kauzya JB, Hayes B, Hayes AC, Thompson JF, Bellerjeau C, et al. 2024. Direct ink writing of viscous inks in variable gravity regimes using parabolic flights. Acta Astronautica 219:569–79
- Kern VR, Sæter T, Carlson A. 2022. Viscoplastic sessile drop coalescence. Phys. Rev. Fluids 7(8):L081601
- Kim YS, Zhu M, Hossain MT, Sanders D, Shah R, et al. 2025. Morphogenic growth 3D printing. Adv. Mater. 37(20):2406265
- Kopatz JW, Reinholtz D, Cook AW, Tappan AS, Grillet AM. 2024. Pressure-based process monitoring of direct-ink write material extrusion additive manufacturing. Addit. Manuf. 80:103928



- Kopatz JW, Unangst J, Cook AW, Appelhans LN. 2021. Compositional effects on cure kinetics, mechanical properties and printability of dual-cure epoxy/acrylate resins for DIW additive manufacturing. Addit. Manuf. 46:102159
- Kulkarni SD, Metzger B, Morris JF. 2010. Particle-pressure-induced self-filtration in concentrated suspensions. Phys. Rev. E 82(1):010402
- Larson R. 1999. The Structure and Rheology of Complex Fluids. Oxford University Press
- Lee CP, Ng MJY, Chian NMY, Hashimoto M. 2024. Multi-material direct ink writing 3D food printing using multi-channel nozzle. *Future Foods* 10:100376
- Legett SA, Torres X, Schmalzer AM, Pacheco A, Stockdale JR, et al. 2022. Balancing functionality and printability: high-loading polymer resins for direct ink writing. *Polymers* 14(21):4661
- Leighton D, Acrivos A. 1987. The shear-induced migration of particles in concentrated suspensions. J. Fluid Mech. 181:415–39
- Lewis J. 2006. Direct ink writing of 3D functional materials. Adv. Funct. Mater. 16(17):2193-204
- Li G, McKinley GH, Ardekani AM. 2015. Dynamics of particle migration in channel flow of viscoelastic fluids. 7. Fluid Mecb. 785:486–505
- Li M, Tian X, Schreyer DJ, Chen X. 2011. Effect of needle geometry on flow rate and cell damage in the dispensing-based biofabrication process. *Biotechnol. Prog.* 27(6):1777–84
- Liu Y, Balmforth N, Hormozi S, Hewitt D. 2016. Two-dimensional viscoplastic dambreaks. J. Non-Newton. Fluid Mech. 238:65-79
- Lohse D. 2022. Fundamental fluid dynamics challenges in inkjet printing. Annu. Rev. Fluid Mech. 54:349-82
- Lozano C, Lumay G, Zuriguel I, Hidalgo R, Garcimartn A. 2012. Breaking arches with vibrations: the role of defects. Phys. Rev. Lett. 109(6):068001
- Malda J, Visser J, Melchels FP, Jüngst T, Hennink WE, et al. 2013. 25th anniversary article: engineering hydrogels for biofabrication. Adv. Mater. 25(36):5011–28
- Marin A, Lhuissier H, Rossi M, Kähler CJ. 2018. Clogging in constricted suspension flows. *Phys. Rev. E* 97(2):021102
- Marin A, Souzy M. 2024. Clogging of noncohesive suspension flows. Annu. Rev. Fluid Mech. 57:89-116
- Marnot A, Koube K, Jang S, Thadhani N, Kacher J, Brettmann B. 2023. Material extrusion additive manufacturing of high particle loaded suspensions: a review of materials, processes and challenges. *Virtual Phys. Prototyp.* 18(1):e2279149
- M'barki A, Bocquet L, Stevenson A. 2017. Linking rheology and printability for dense and strong ceramics by direct ink writing. Sci. Rep. 7(1):6017
- McKenzie R, Koerner H. 2020. Enabling direct writing of an epoxy resin with thermo-activated organic thixotropes. *Addit. Manuf.* 31:100905
- Mechtcherine V, Bos FP, Perrot A, Leal da Silva W, Nerella V, et al. 2020. Extrusion-based additive manufacturing with cement-based materials production steps, processes, and their underlying physics: a review. Cement Concrete Res. 132:106037
- Mewis J, Wagner NJ. 2011. Colloidal Suspension Rheology. Cambridge University Press
- Mezi D, Ausias G, Grohens Y, Férec J. 2019. Numerical simulation and modeling of the die swell for fiber suspension flows. *7. Non-Newton. Fluid Mech.* 274:104205
- Mitsoulis E, Vlachopoulos J, Mirza F. 1984. Numerical simulation of entry and exit flows in slit dies. *Polymer Eng. Sci.* 24(9):707–15
- Mondal S, Wu C-H, Sharma MM. 2016. Coupled CFD-DEM simulation of hydrodynamic bridging at constrictions. *Int. 7. Multiphase Flow* 84:245–63
- Moore CP, Husson J, Boudaoud A, Amselem G, Baroud CN. 2023. Clogging of a rectangular slit by a spherical soft particle. *Phys. Rev. Lett.* 130(6):064001
- Morris SW, Dawes JH, Ribe NM, Lister JR. 2008. Meandering instability of a viscous thread. *Phys. Rev. E* 77(6):066218
- Münstedt H. 2018. Extensional rheology and processing of polymeric materials. *Int. Polymer Proc.* 33(5):594–618
- Murphy SV, Atala A. 2014. 3D bioprinting of tissues and organs. Nat. Biotechnol. 32(8):773-85
- Muth JT, Vogt DM, Truby RL, Mengüç Y, Kolesky DB, et al. 2014. Embedded 3D printing of strain sensors within highly stretchable elastomers. *Adv. Mater.* 26(36):6307–12





- Najmon JC, Raeisi S, Tovar A. 2019. Review of additive manufacturing technologies and applications in the aerospace industry. Addit. Manuf. Aerospace Ind. 2019:7-31
- Nelson AZ, Bras RE, Liu J, Ewoldt RH. 2018. Extending yield-stress fluid paradigms. 7. Rheol. 62(1):357-69 Nelson AZ, Ewoldt RH. 2017. Design of yield-stress fluids: a rheology-to-structure inverse problem. Soft Matter 13(41):7578-94
- Nelson AZ, Schweizer KS, Rauzan BM, Nuzzo RG, Vermant J, Ewoldt RH. 2019. Designing and transforming yield-stress fluids. Curr. Opin. Solid State Mater. Sci. 23(5):100758
- Ng A, Telles R, Riley KS, Lewis JA, Cook CC, et al. 2025. Coaxial direct ink writing of cholesteric liquid crystal elastomers in 3D architectures. Adv. Mater. 37(10):2416621
- Ngo T, Kashani A, Imbalzano G, Nguyen K, Hui D. 2018. Additive manufacturing (3D printing): a review of materials, methods, applications and challenges. Composites Part B Eng. 143:172-96
- Ouyang L, Armstrong JP, Lin Y, Wojciechowski JP, Lee-Reeves C, et al. 2020. Expanding and optimizing 3D bioprinting capabilities using complementary network bioinks. Sci. Adv. 6(38):eabc5529
- Pack RC, Romberg SK, Badran AA, Hmeidat NS, Yount T, Compton BG. 2020. Carbon fiber and syntactic foam hybrid materials via core-shell material extrusion additive manufacturing. Adv. Mater. Technol. 5(12):2000731
- Pandya KS, Shindalkar SS, Kandasubramanian B. 2023. Breakthrough to the pragmatic evolution of direct ink writing: progression, challenges, and future. Progress Addit. Manuf. 8(6):1303-28
- Paolini A, Kollmannsberger S, Rank E. 2019. Additive manufacturing in construction: a review on processes, applications, and digital planning methods. Addit. Manuf. 30:100894
- Pashias N, Boger D, Summers J, Glenister D. 1996. A fifty cent rheometer for yield stress measurement. 7. Rheol. 40(6):1179-89
- Pednekar S, Chun J, Morris JF. 2018. Bidisperse and polydisperse suspension rheology at large solid fraction. 7. Rheol. 62(2):513-26
- Pettas D, Karapetsas G, Dimakopoulos Y, Tsamopoulos J. 2015. On the origin of extrusion instabilities: linear stability analysis of the viscoelastic die swell. 7. Non-Newton. Fluid Mech. 224:61-77
- Placone JK, Engler AJ. 2018. Recent advances in extrusion-based 3D printing for biomedical applications. Adv. Healthcare Mater. 7(8):1701161
- Rajesh S, Thiévenaz V, Sauret A. 2022. Transition to the viscoelastic regime in the thinning of polymer solutions. Soft Matter 18(16):3147-56
- Rane K, Strano M. 2019. A comprehensive review of extrusion-based additive manufacturing processes for rapid production of metallic and ceramic parts. Adv. Manuf. 7(2):155-73
- Rau DA, Williams CB, Bortner MJ. 2023. Rheology and printability: a survey of critical relationships for direct ink write materials design. Prog. Mater. Sci. 140:101188
- Ribe NM, Habibi M, Bonn D. 2012. Liquid rope coiling. Annu. Rev. Fluid Mech. 44:249-66
- Ribeiro A, Blokzijl MM, Levato R, Visser CW, Castilho M, et al. 2017. Assessing bioink shape fidelity to aid material development in 3D bioprinting. Biofabrication 10(1):014102
- Romberg SK, Abir AI, Hershey CJ, Kunc V, Compton BG. 2022a. Structural stability of thin overhanging walls during material extrusion additive manufacturing of thermoset-based ink. Addit. Manuf. 53:102677
- Romberg SK, Hershey CJ, Lindahl JM, Carter WG, Condon J, et al. 2022b. Large-scale reactive thermoset printing: complex interactions between temperature evolution, viscosity, and cure shrinkage. Int. J. Adv. Manuf. Technol. 123(9):3079-94
- Romberg SK, Islam MA, Hershey CJ, DeVinney M, Duty CE, et al. 2021. Linking thermoset ink rheology to the stability of 3D-printed structures. Addit. Manuf. 37:101621
- Rothstein JP, McKinley GH. 2001. The axisymmetric contraction-expansion: the role of extensional rheology on vortex growth dynamics and the enhanced pressure drop. J. Non-Newton. Fluid Mech. 98(1):33-63
- Saadi M, Maguire A, Pottackal NT, Thakur MSH, Ikram MM, et al. 2022. Direct ink writing: a 3D printing technology for diverse materials. Adv. Mater. 34(28):2108855
- Saengow C, Sen S, Yus J, Lovrich EE, Hoika AG, et al. 2025. Stretching the printability metric in direct-ink writing with highly extensible yield-stress fluids. Preprint, arXiv:2501.12630v1 [cond-mat.soft]
- Sauret A, Barney EC, Perro A, Villermaux E, Stone HA, Dressiare E. 2014. Clogging by sieving in microchannels: application to the detection of contaminants in colloidal suspensions. Appl. Phys. Lett. 105(7):074101

- Schaffner M, Rühs PA, Coulter F, Kilcher S, Studart AR. 2017. 3D printing of bacteria into functional complex materials. Sci. Adv. 3(12):eaao6804
- Schild T, Cowley A, Grundström B, Garrivier N, Hensch N. 2024. Direct ink writing with lunar regolith: an avenue for off-Earth construction. In Adaptive On- and Off-Earth Environments, ed. A Cervone, H Bier, A Makaya. Springer International Publishing
- Schuller T, Jalaal M, Fanzio P, Galindo-Rosales FJ. 2024. Optimal shape design of printing nozzles for extrusion-based additive manufacturing. *Addit. Manuf.* 84:104130
- Schwab A, Levato R, D'Aoèste M, Piluso S, Eglin D, Malda J. 2020. Printability and shape fidelity of bioinks in 3D bioprinting. *Chem. Rev.* 120(19):11028–55
- Skylar-Scott MA, Uzel SG, Nam LL, Ahrens JH, Truby RL, et al. 2019. Biomanufacturing of organ-specific tissues with high cellular density and embedded vascular channels. Sci. Adv. 5(9):eaaw2459
- Smay JE, Cesarano J, Lewis JA. 2002. Colloidal inks for directed assembly of 3-D periodic structures. *Langmuir* 18(14):5429-37
- Staron L, Lagrée P-Y, Ray P, Popinet S. 2013. Scaling laws for the slumping of a Bingham plastic fluid. 7. Rheol. 57(4):1265–80
- Stickel JJ, Powell RL. 2005. Fluid mechanics and rheology of dense suspensions. *Annu. Rev. Fluid Mech.* 37:129–49
- Tagliaferri S, Panagiotopoulos A, Mattevi C. 2021. Direct ink writing of energy materials. *Mater. Adv.* 2(2):540–63
- Tang D, Marchesini FH, Cardon L, D'hooge DR. 2020. State of the-art for extrudate swell of molten polymers: from fundamental understanding at molecular scale toward optimal die design at final product scale. *Macromol. Mater. Eng.* 305(11):2000340
- Tanner R. 1970. A theory of die-swell. J. Polym. Sci. Part A-2 Polym. Phys. 8(12):2067-78
- Tay RY, Song Y, Yao DR, Gao W. 2023. Direct-ink-writing 3D-printed bioelectronics. Mater. Today 71:135-51
- Teves S, Biermann T, Ziebehl A, Eckert JG, Hill O, et al. 2024. Active-mixing printhead for on-the-fly composition adjustment of multi component materials in direct ink writing. *Addit. Manuf. Lett.* 10:100217
- Therriault D, White SR, Lewis JA. 2007. Rheological behavior of fugitive organic inks for direct-write assembly. *Appl. Rheol.* 17(1):10112
- Thiévenaz V, Rajesh S, Sauret A. 2021. Droplet detachment and pinch-off of bidisperse particulate suspensions. *Soft Matter* 17(25):6202–11
- Thiévenaz V, Sauret A. 2021. Pinch-off of viscoelastic particulate suspensions. *Phys. Rev. Fluids* 6(6):L062301 Thiévenaz V, Sauret A. 2022a. Fragmentation of viscous compound liquid ligaments. *Phys. Rev. Fluids* 7(11):110501
- Thiévenaz V, Sauret A. 2022b. The onset of heterogeneity in the pinch-off of suspension drops. *PNAS* 119(13):e2120893119
- Tian X, Zhou K. 2020. 3D printing of cellular materials for advanced electrochemical energy storage and conversion. *Nanoscale* 12(14):7416–32
- Tirtaatmadja V, Sridhar T. 1993. A filament stretching device for measurement of extensional viscosity. J. Rheol. 37(6):1081–102
- Uitz O, Koirala P, Tehrani M, Seepersad CC. 2021. Fast, low-energy additive manufacturing of isotropic parts via reactive extrusion. *Addit. Manuf.* 41:101919
- van der Kolk J, Tieman D, Jalaal M. 2023. Viscoplastic lines: printing a single filament of yield stress material on a surface. *J. Fluid Mech.* 958:A34
- Vani N, Escudier S, Jeong DH, Sauret A. 2024. Role of the constriction angle on the clogging by bridging of suspensions of particles. Phys. Rev. Rev. 6(3):L032060
- Vani N, Escudier S, Sauret A. 2022. Influence of the solid fraction on the clogging by bridging of suspensions in constricted channels. Soft Matter 18(36):6987–97
- Villalba ME, Daneshi M, Martinez DM. 2023. Characterizing jamming of dilute and semi-dilute fiber suspensions in a sudden contraction and a T-junction. Phys. Fluids 35(12):123339
- Wang T-p, Shen L, Forrester M, Lee T-H, Torres S, et al. 2024. Shelf-stable Bingham plastic polyurethane thermosets for additive manufacturing. *ACS Mater. Lett.* 6(3):1077–85
- Wei P, Cipriani C, Hsieh C-M, Kamani K, Rogers S, Pentzer E. 2023. Go with the flow: rheological requirements for direct ink write printability. *J. Appl. Phys.* 134(10):100701

- Wilt JK, Gilmer D, Kim S, Compton BG, Saito T. 2021. Direct ink writing techniques for in situ gelation and solidification. MRS Commun. 11:106–21
- Wu Q, Song K, Zhang D, Ren B, Sole-Gras M, et al. 2022. Embedded extrusion printing in yield-stress-fluid baths. *Matter* 5(11):3775–806
- Wu SJ, Wu J, Kaser SJ, Roh H, Shiferaw RD, et al. 2024. A 3D printable tissue adhesive. *Nat. Commun.* 15(1):1215
- Wyss HM, Blair DL, Morris JF, Stone HA, Weitz DA. 2006. Mechanism for clogging of microchannels. *Phys. Rev. E* 74(6):061402
- Yirmibesoglu OD, Simonsen LE, Manson R, Davidson J, Healy K, et al. 2021. Multi-material direct ink writing of photocurable elastomeric foams. *Commun. Mater.* 2(1):82
- Yuk H, Zhao X. 2018. A new 3D printing strategy by harnessing deformation, instability, and fracture of viscoelastic inks. Adv. Mater. 30(6):1704028
- Zhang H, Zhang L, Zhang H, Wu J, An X, Yang D. 2021. Fibre bridging and nozzle clogging in 3D printing of discontinuous carbon fibre-reinforced polymer composites: coupled CFD-DEM modelling. Int. J. Adv. Manuf. Technol. 117(11):3549–62
- Zhang P, Lei IM, Chen G, Lin J, Chen X, et al. 2022. Integrated 3D printing of flexible electroluminescent devices and soft robots. *Nat. Commun.* 13(1):4775
- Zhao Y, Yu P, Tao Y, Zhang X, Li M, et al. 2025. Long-term stability and durability of direct-ink-writing 3D-printed sensors: challenges, strategies and prospects. *Virtual Phys. Prototyp.* 20(1):e2460211
- Zhu Y, Liu N, Chen Z, He H, Wang Z, et al. 2023. 3D-printed high-frequency dielectric elastomer actuator toward insect-scale ultrafast soft robot. ACS Mater. Lett. 5(3):704–14
- Ziaee M, Naseri I, Johnson JW, Franklin KA, Yourdkhani M. 2023. Frontal polymerization and threedimensional printing of thermoset polymers with tunable thermomechanical properties. ACS Appl. Polym. Mater. 5(3):1715–24
- Zocca A, Colombo P, Gomes CM, Günster J. 2015. Additive manufacturing of ceramics: issues, potentialities, and opportunities. J. Am. Ceram. Soc. 98(7):1983–2001